الجـــمـــهـــوريـــة الجـزائـريـة الديمـقـراطيـة الـشـعـبيـة

PEOPLE'S DEMOCRATIC REPUBLIC OF ALGERIA

وزارة التـــعـــليـــم العــــــالي والبــــحث العــــــلـــمــــي

MINISTRY OF HIGHER EDUCATION AND SCIENTIFIC RESEARCH

جـــــــــــــامعة سعيدة – د. الطاهر مولاي –

University of Saïda – Dr. Tahar Moulay –

Faculty of Mathematics, Computer Science and Telecommunications

DISSERTATION

Presented for the attainment of **Master's Degree in Telecommunications**

Specialty: Networks and Telecommunications

By: Mr. BOUKHATEM Alaa Eddine
Miss. KRATTOU Hadjer

Design and Optimization of Miniaturized SIW/HMSIW Based Bandpass Filters for Diverse Applications

Defended on June 19th, 2025, before the jury composed of:

Dr. BOUDKHIL Abdelhakim	MCA	President
Dr. BOUBAKAR Hichem	MCB	Supervisor
Dr. BELHADJ Salima	MCB	Examiner

2024 / 2025

Acknowledgement

Above all, our gratitude and thanks go to Allah Who has given us health, strength, patience, courage and the Will to finish this work.

Our sincere thanks go to our supervisor Dr. BOUBAKAR HICHEM for his guidance and scientific advice throughout this work.

Also

Our thanks go to the members of the jury for having honored and for the effort made to judge this modest work.

Our thanks also go to all our teachers who have contributed to our training.

Abstract

This dissertation presents the design and analysis of advanced bandpass filters utilizing Substrate Integrated Waveguide (SIW) and Half-Mode SIW (HMSIW) technologies, addressing the demand for compact, high-performance microwave components. A novel Complementary Hexagonal Metamaterial Cell (CHMC) is introduced and strategically integrated into these platforms, demonstrating significant filter miniaturization while maintaining low insertion loss and good out-of-band rejection. The versatility of the CHMC enabled the development of narrow-band, wider-bandwidth single-band, and dual-band filters, with its metamaterial behavior validated by negative refractive index extraction. The findings establish the CHMC as an effective and adaptable building block for high-performance microwave filters crucial for modern communication systems.

Keywords: bandpass filters, SIW, HMSIW, CHMC, Metamaterial.

ملخص

قدم هذه الرسالة تصميم وتحليل مرشحات تمرير النطاق المتقدمة باستخدام تقنيات موجه الموجات المدمج في الركيزة (SIW) ونصف النمط لموجه الموجات المدمج في الركيزة (HMSIW)، استجابةً للطلب على مكونات الموجات الدقيقة المدمجة وعالية الأداء. يتم تقديم خلية مواد خارقة سداسية تكميلية مبتكرة (CHMC) ودمجها بشكل استراتيجي في هذه المنصات، مما يُظهر تصغيرًا كبيرًا للمرشحات مع الحفاظ على خسارة إدخال منخفضة ورفض جيد خارج النطاق. مكّن تعدد استخدامات CHMC من تطوير مرشحات ضيقة النطاق، وأحادية النطاق ذات نطاق ترددي أوسع، وثنائية النطاق، مع التحقق من سلوكها كمادة خارقة (metamaterial) من خلال استخلاص معامل انكسار سالب. تثبت النتائج أن CHMC تشكل لبنة بناء فعالة وقابلة للتكيف لمرشحات الموجات الدقيقة عالية الأداء، وهي حاسمة لأنظمة الاتصالات الحديثة.

كلمات مفتاحية: مرشحات النطاق الترددي، SIW، HMSIW، CHMC، مواد خارقة.

Résumé

Ce mémoire présente la conception et l'analyse de filtres passe-bande avancés utilisant les technologies de Guide d'Ondes Intégré au Substrat (SIW) et Demi-Mode SIW (HMSIW), répondant à la demande de composants hyperfréquences compactes et à haute performance. Une nouvelle Cellule Métamatériau Hexagonale Complémentaire (CHMC) est introduite et intégrée de manière stratégique dans ces plateformes, démontrant une miniaturisation significative des filtres tout en maintenant de faibles pertes d'insertion et une bonne réjection hors bande. La polyvalence de la CHMC a permis le développement de filtres à bande étroite, à bande plus large monobande, et bibandes, son comportement de métamatériau étant validé par l'extraction d'un indice de réfraction négatif. Les résultats établissent la CHMC comme un élément de base efficace et adaptable pour les filtres hyperfréquences à haute performance essentiels aux systèmes de communication modernes.

Mots clés : Filtres Passe-Bande, SIW, HMSIW, CHMC, Métamatériau.

Table of Contents

Chapter II: SIW and HMSIW techniques

Chapter III: SIW/HMSIW bandpass filters loaded with CHMCs

List of Figures

Chapter I: Theory and design of filters

Chapter II: SIW and HMSIW techniques

Chapter III: SIW/HMSIW bandpass filters loaded with CHMCs

List of Tables

List of Abbreviations

BPF:	Bandpass Filter
CHMC:	Complementary Hexagonal Metamaterial Cell
CPW:	Coplanar Waveguide
CSRR:	Complementary Split-Ring Resonator
CST:	Computer Simulation Technology
DGS:	Defected Ground Structure
HFSS:	High-Frequency Structure Simulator
HMSIW:	Half-Mode Substrate Integrated Waveguide
MMT:	Metamaterial
NRW:	Nicolson-Ross-Weir
QE:	External quality factor
QL:	Loaded quality factor
QU:	Unloaded quality factor
RF:	Radio Frequency
RWG:	Rectangular Waveguide
SIW:	Substrate Integrated Waveguide
SRR:	Split-Ring Resonator
TE:	Transverse Electrical
TEM:	Transverse Electromagnetic
TM:	Transverse Magnetic
WIFI:	Wireless fidelity
WiMAX:	Worldwide Interoperability for Microwave Access
WLAN:	Wireless Local Area Network

GENERAL INTRODUCTION

General Introduction

Telecommunication systems have become an indispensable fabric of modern society, underpinning global communication, data exchange, and technological advancement. Central to the efficient and reliable operation of these systems are microwave filters. These components play a critical role in signal processing by selectively allowing frequencies within a specific band to pass while attenuating undesired frequencies. This selective filtering is crucial for managing the increasingly crowded electromagnetic spectrum, preventing interference between different communication channels, and ensuring the integrity of transmitted and received signals. The performance of filters, characterized by parameters such as insertion loss, return loss, bandwidth, and out-of-band rejection, directly impacts the overall quality and efficiency of the entire telecommunication system.

As the demand for higher data rates, increased capacity, and more compact devices continues to grow, traditional filter technologies like microstrip lines and conventional waveguides face significant challenges. While microstrip technology offers planarity and ease of integration, it often suffers from higher insertion loss and limited power handling capabilities, especially at higher frequencies. Conversely, conventional metallic waveguides provide excellent performance in terms of low loss and high power handling but are typically bulky, expensive, and difficult to integrate with planar circuits. To bridge this gap, Substrate Integrated Waveguide (SIW) technology has emerged as a highly promising solution. SIW structures effectively emulate the performance of rectangular waveguides by embedding them within a dielectric substrate using rows of metallic vias, thereby merging the low-loss, high-quality factor (Q-factor), and good power handling capabilities of traditional waveguides with the planar profile, ease of fabrication, and integration benefits of microstrip circuits. This synergy makes SIW an attractive platform for a wide array of high-frequency components.

Building upon the advantages of SIW, Half-Mode Substrate Integrated Waveguide (HMSIW) technology offers a further step towards miniaturization. By effectively bisecting the SIW structure along a magnetic wall, HMSIW components can achieve approximately half the size of their full-mode SIW counterparts, often with minimal degradation in performance. This size reduction is particularly valuable in applications where space is at a premium, such as in portable devices, satellite communications, and densely packed integrated circuits, without significantly compromising the desirable electromagnetic properties of SIW.

In this context, the present work focuses on the exploration and development of bandpass filters utilizing both SIW and HMSIW technologies. A number of innovative filter designs are presented and analyzed through simulation. A key aspect of this research involves the introduction and application of a novel metamaterial structure, termed the Complementary Hexagonal Metamaterial Cell (CHMC), which is based on hexagonal complementary split ring resonators (CSRRs). The unique properties of these CHMC cells are leveraged to achieve enhanced filter performance, particularly in terms of miniaturization and tailored frequency responses.

This dissertation is organized as follows:

- **Chapter I** introduces the general background on microwave filters, discussing their fundamental principles, classifications, key performance parameters, and the evolution of filter technologies, thereby setting the stage for the specialized topics addressed in subsequent chapters.
- **Chapter II** presents Substrate Integrated Waveguide (SIW) and Half-Mode Substrate Integrated Waveguide (HMSIW) technologies in detail. It will cover their operating principles, design methodologies, inherent advantages, and their effective use in designing various high-frequency electromagnetic components.
- **Chapter III** forms the core of this research, presenting the design, simulation, and analysis of a number of bandpass filters. This chapter details filters based on both SIW and HMSIW platforms, with a significant focus on the incorporation of the newly proposed Complementary Hexagonal Metamaterial Cell (CHMC). The influence of CHMC configurations on filter miniaturization, bandwidth, and overall performance, including single-band and dual-band applications, will be thoroughly investigated.

CHAPTER I

Theory and design of filters

I.1. Introduction

The evolving landscape of high-frequency and microwave engineering, filters serve as indispensable components for spectrum control and signal integrity in modern communication systems. The stringent requirements for selectivity, compactness, and low loss in applications such as telecommunications, radar, and satellite communication have driven significant advancements in filter design. Traditional waveguide structures, known for their high-quality factor and power handling capabilities, often suffer from bulky form factors and high manufacturing costs [I.1-I.3]. To overcome these limitations [I.4], planar technologies have gained prominence due to their compatibility with integrated circuit fabrication [I.5], compact size [I.5- I.7], and cost-effectiveness [I.7- I.11].

This chapter provides a comprehensive theoretical foundation for microwave filter design. It outlines wave propagation in various guide types, introduces essential filter classifications and synthesis methods, and discusses their electrical parameters and approximation techniques.

I.2. Waveguide technology

The waveguides are transmission lines used for the guidance of an electromagnetic signal by reflection on the internal walls of the guide (Figure I.1). Many techniques are used for the realization of waveguides "waves. We can distinguish two main families of waveguide manufacturing technology: volume technology and planar technology.

I.2.1 Volume technology

For this type of guides, the action is put on the manufacturing and realization technology. For this, we can distinguish two types of waveguides in volume technology: rectangular waveguides and circular waveguides.

I.2.1.1 The rectangular waveguide

The rectangular waveguide is one of the first types of transmission lines used to transport microwave signals. Several components, such as couplers, phase shifters, or attenuators are commercially available for frequencies from 1 GHz to more than 220 GHz. Although microwave circuits are becoming more and more miniaturized, rectangular guides are still used because of their ability to transport high powers [I.12].

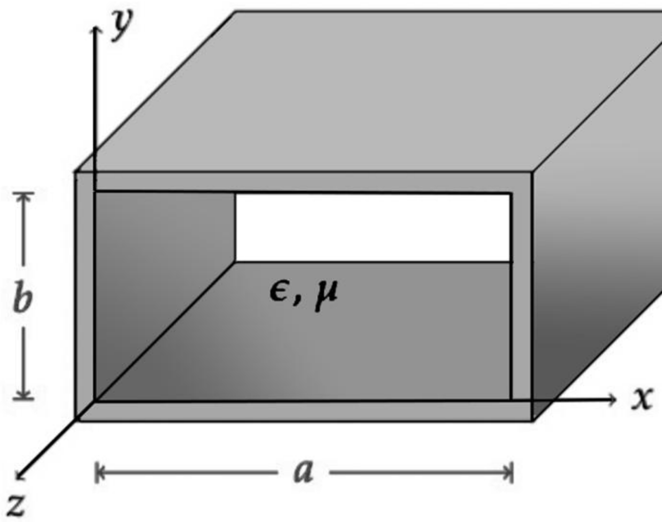

Figure I.1: Rectangular waveguide.

Figure I.1 shows an example of a rectangular waveguide. It is assumed that the guide is filled with a dielectric having a permittivity ε and a permeability µ. By convention, the longest side of the guide is on the x axis, which gives a>b.

The representation of the electromagnetic field in a rectangular waveguide governed by Maxwell's equations [I.12] which are given:

We note:

$$\overrightarrow{rot} = -\frac{\partial \overrightarrow{B}}{\partial t} \qquad \text{(I. 1)}$$

$$\overrightarrow{rot}\,\overrightarrow{B} = \mu_0 \underset{j}{\rightarrow} + \varepsilon_r \varepsilon_0\, \mu_0 \frac{\overrightarrow{\partial E}}{\partial t} \qquad \text{(I.2)}$$

$$div\,\overrightarrow{E} \;=\; \frac{\rho}{\varepsilon} \qquad \text{(I. 3)}$$

$$\overrightarrow{d\iota v}\,\overrightarrow{H} = \; 0 \qquad \text{(I. 4)}$$

ρ:The volume density of electric charge.

$\vec{j}$: The current density vector.

$\vec{E}$: The electric field vector.

$\overrightarrow{B}$: The pseudo-vector magnetic induction.

ε_0 : The dielectric permittivity of the vacuum.

μ_0: The magnetic permeability of the vacuum.

The equations of propagation of electric $\vec{E}$ and magnetic $\vec{H}$ fields are:

$$\nabla^2\vec{E} + \omega^2\varepsilon\mu\vec{E} = 0 \qquad (\text{I}.5)$$

$$\nabla^2\vec{H} + \omega^2\varepsilon\mu H = 0 \qquad (\text{I}.6)$$

On which this wave will be reflected successively. We can express the fields in the form:

$$\vec{E}\,(x,y,z,t) = \vec{E}(x,y)e^{-j\omega t\gamma z} \qquad (\text{I.7})$$

$$\vec{H}(x,y,z,t) = \vec{H}(x,y)e^{-j\omega t\gamma z} \qquad (1.8)$$

$$\text{with: } \gamma = \alpha + j\beta g \qquad (I.9)$$

Where:

α and βg represent respectively the attenuation and the longitudinal propagation constant.

K represents the propagation constant in the dielectric medium in which the wave propagates at speed *v*:

$$k^2=\omega^2\varepsilon\mu \qquad (\text{I.10})$$

$$v = \frac{1}{\sqrt{\varepsilon_r\mu_r\varepsilon_0\mu_0}} \qquad (\text{I.11})$$

In it the speed of light in the air given by:

$$c = \frac{1}{\sqrt{\varepsilon_0\mu_0}} = 3\ 10^8 m/s \qquad (\text{I.12})$$

The equations (I.8) and (I.9) injected respectively in (I.5) and (I.6) give:

$$\nabla_t^2 \vec{E} + (k^2 + \gamma^2)\vec{E} = 0 \qquad (I.13)$$

$$\nabla_t^2 \vec{H} + (k^2 + \gamma^2)\vec{H} \qquad (I.14)$$

Such as:

∇^2 Presents the transverse La placian given by:

$$\nabla_t^2 = \frac{\partial^2}{\partial_x^2} + \frac{\partial^2}{\partial_y^2} \qquad (I.15)$$

We find three types of propagation mode for a rectangular waveguide.

The transverse electric wave TE characterized by Ez=0 and Hz= 0.

The transverse magnetic wave TM characterized by Hz=0 and Ez≠0.

The hybrid wave characterized by Ez≠0 and Hz≠ 0.

The electromagnetic transverse mode TEM (Ez=Hz=0) cannot exist in a closed guide because of its walls which form a plane perpendicular to the direction of propagation.

I.2.1.1.a Study of TE mode

In the case of propagation of TE modes, we have: $E_z(x,y)=0$ et $H_z \neq 0$. (I.16)

H(x, y) must satisfy $\frac{\partial^2 H_z}{\partial x^2} + \frac{\partial^2 H_z}{\partial y^2} + K^2 H_z = 0 \; with \; \frac{\partial H_z}{\partial n} = 0$ (I.17)

The solution Hz is "written in the form :

$$H_z(x,y) = H_0 \cos\left(\frac{m\pi x}{a}\right) \cos\left(\frac{m\pi y}{b}\right) e^{-\alpha z} e^{-j(\omega - \beta z)} \qquad (I.18)$$

$$H_z(x,y) = H_z^* \cos\left(\frac{m\pi x}{a}\right) \cos\left(\frac{m\pi y}{b}\right) \qquad (I.19)$$

$$K_c^2 = \left(\frac{m\pi}{a}\right)^2 + \left(\frac{m\pi}{b}\right)^2 \qquad (I.20)$$

From these relations it is possible to deduce all the components of the TE modes existing in the rectangular waveguide, that is to say the TE_{mn} modes with m and n positive integers translating the number of extremisms of the electromagnetic field respectively in the x and y directions.

The expressions of the electromagnetic field of these modes are as follows:

$$Ex(x,y) = H_z^* \frac{j\omega\varepsilon}{K^2} \frac{n\pi}{b} cos\left(\frac{m\pi x}{a}\right) sin\left(\frac{n\pi y}{b}\right) \tag{I.21}$$

$$Ex(x,y) = -H_0^* \frac{j\omega\varepsilon}{K^2} \frac{m\pi}{b} cos\left(\frac{m\pi x}{a}\right) sin\left(\frac{n\pi y}{b}\right) \tag{I.22}$$

$$Ez(x,y) = 0 \tag{I.23}$$

$$Hx(x,y) = H_0^* \frac{y}{K^2} \frac{m\pi}{b} sin\left(\frac{m\pi x}{a}\right) cos\left(\frac{n\pi y}{b}\right) \tag{I.24}$$

$$Hy \quad (x,y) = H_0^* \frac{y}{K^2} \frac{n\pi}{b} cos \frac{m\pi x}{a} sin \frac{n\pi y}{b} \tag{I.25}$$

$$Hz \quad (x,y) = H_z^* \cos\left(\frac{m\pi x}{a}\right) \sin\left(\frac{n\pi y}{b}\right) \tag{I.26}$$

I.2.1.1.b Study of TM modes

The TM waves are characterized by Hz =0 and Ez ≠0, such that the magnetic field only is orthogonal to the propagation axis.

E(*x*,*y*) must satisfy:

$$\frac{\partial^2 E_z}{\partial x^2} + \frac{\partial^2 E_z}{\partial y^2} + K^2 E_z = 0 \tag{I.27}$$

With E_z=0 on the walls of the guide.

For a width of the guide a and a height b, the continuity conditions on the walls of the guide allow us to extract the expression of different components of the wave fields:

$$Ez \quad (x,y) = E_0^* \sin\left(\frac{m\pi x}{a}\right) \sin\left(\frac{n\pi y}{b}\right) \tag{I.28}$$

$$Ex \quad (x,y) = -E_0^* \frac{y}{K^2} \frac{m\pi}{a} \cos\left(\frac{m\pi x}{a}\right) \sin\left(\frac{n\pi y}{b}\right) \tag{I.29}$$

$$Ey \quad (x,y) = -E_0^* \frac{y}{K^2} \frac{n\pi}{a} \sin\left(\frac{m\pi x}{a}\right) \cos\left(\frac{n\pi y}{b}\right) \tag{I.30}$$

$$Hx \quad (x,y) = E_0^* \frac{j\omega\varepsilon}{K^2} \frac{n\pi}{b} \sin\left(\frac{m\pi x}{a}\right) \cos\left(\frac{n\pi y}{b}\right) \tag{I.31}$$

$$Hy \quad (x,y) = -E_0^* \frac{j\omega\varepsilon}{K^2} \frac{m\pi}{a} \cos\left(\frac{m\pi x}{a}\right) \sin\left(\frac{n\pi y}{b}\right) \qquad \text{(I.32)}$$

I.2.1.1.c The cut-off frequency and the fundamental modes

A wave of frequency f can propagate in the TE_{mn} or TM_{mn} si:

$$f > f_c = \frac{v}{2}\sqrt{\frac{m^2}{a^2} + \frac{n^2}{b^2}} \qquad \text{(I.33)}$$

With: f_c the cut-off frequency of the mode TE_{mn} or TM_{mn}.

this cut-off frequency depends not only on the dielectric which is located in the rectangular guide but also on the dimensions a and b of the guide.

We call the fundamental mode the one that represents the smallest cut-off frequency $f_{c_{mn}}$. The ranking of the modes TE_{mn} is obtained from the calculation of the cut-off frequencies $f_{c_{mn}}$. For the mode TE_{mn} and $a>b$ the fundamental mode of a rectangular waveguide is the TE_{10} mode.

For the mode TM_{mn}, the modes TM_{00}, TM_{10} and TM_{01} don't exist. The fundamental mode which can propagate is the TM11 mode (Figure I.2.).

I.2.1.1.d The field lines

In the figure below we present the field figures of the TE10 mode in a rectangular waveguide.

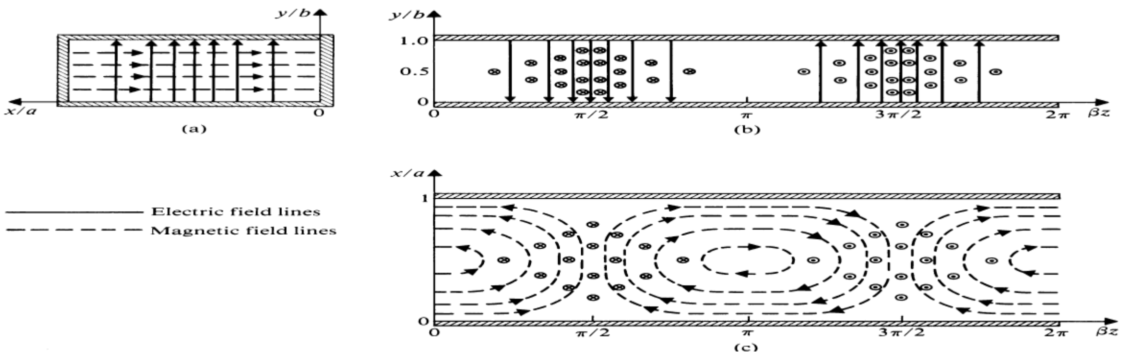

Figure I.2: Field lines of the TE10 mode in a rectangular guide [I.12].

I.2.2 Planar technology

Planar technologies are complementary to volumetric technologies. Where the latter struggle because of their excessive bulk and weight, or because of their poor connectivity, planar technologies respond favorably to these criteria. They are also adapted to mass production, and therefore to cost reduction. These qualities have a price that is paid by allowable powers limited to Watt.

The principle is based on the use of a dielectric substrate in the form of plates, metallized on one or both sides. Several designs are then possible, such as for example micro-strip lines, co-planars or tri-plates.

I.2.2.1 The micro-strip line

The micro-strip lines [I.13] are the most widely used lines for designing high-frequency integrated circuits. The geometry is shown in Figure I.3. A conductive strip of width W is printed on a substrate of thickness h with a relative permittivity ε_r, the other face of which constitutes a ground plane.

The mastery of this technology makes the costs much lower than for volume technologies, as well as its good connectivity, its small footprint and its small volume make it an ideal candidate to be included in the other modules.

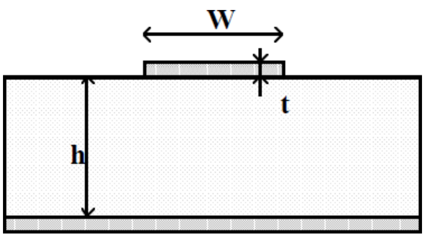

Figure I.3: presentation of a micro-ribbon line.

The propagation of the waves in this inhomogeneous structure takes place partly in the dielectric, partly in the air, the proportion depends on the dielectric constant value of the substrate.

The Characteristics of micro-ribbon line

The following characteristics can be mentioned:

- Both alternating current and direct current signals can be transmitted.

- Active components, diodes and transistors can be easily implemented (branch connections are also easily achievable). The characterization of the components on the circuit is simple to perform.
- The wavelength of the line is considerably reduced (usually a third of its value in a vacuum).
- The structure is quite irregular and can withstand moderately high voltages and power levels.

The advantages and disadvantages of micro-ribbon lines

The following advantages can be mentioned:

- Any configuration of the upper conductor can be deposited directly on the dielectric which is an inexpensive operation.
- Semiconductor elements can be easily attached to this structure since it's of plane configuration.
- All the elements incorporated into the structure are generally accessible.

But despite these performances they have disadvantages that can be cited:

- The losses are higher as a result of the radiation; they strongly depend on the thickness and the dielectric constant of the substrate.
- The electric field is disturbed by the air-dielectric interface.
- Existence of an edge effect: the fields extend on both sides of the ribbon.
- The electric and magnetic fields are orthogonal in the transverse plane.

I.2.2.2 The coplanar lines

The structure of the coplanar line coincides with the same structure as that of the micro-strip line. It's another type of waveguide used for integrated circuits.

The coplanar technology is materialized by a metallization on a single substrate face. The line is then materialized by two slots engraved in the metal, as shown in Figure I.4. This technology has the advantage of further reducing the manufacturing cost since everything is made on a single face. We thus get rid of the additional bores and metal deposits. However, the fact of having three conductors in parallel makes the propagation possible according to two fundamental modes. The first is the quasi-TEM mode, and the second is the TE mode. The latter appears in particular with the presence of discontinuities. The solution to get rid of the TE mode consists in putting the two metal planes external to the line at the same potential. But in practice, this remains difficult and expensive to achieve. For this reason, the coplanar remained little used.

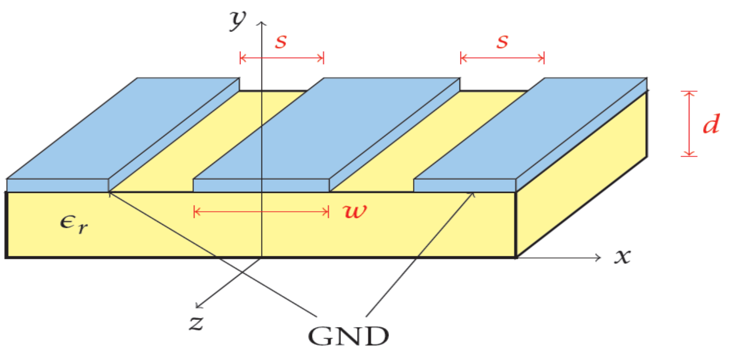

Figure I.4: Presentation of a coplanar line.

I.2.2.3 The tri-plate technology

The tri-plate technology amounts to embedding a metal strip in a substrate, the two faces of which have been metalized. We therefore find, as for the coplanar, three conductors in parallel, with two possible propagation modes. But unlike the coplanar, the parasitic mode can be easily eliminated by adding metalized vias throughout the line, to connect the two metallized faces and maintain them at the same electrical potential. In addition, the fact of embedding the line in a substrate makes it possible to considerably reduce the dimensions thanks to a higher relative permittivity. Moreover, the metallization of the two faces protects against radiation losses.

The disadvantages of tri-plate are to have higher realization costs than other planar techniques, and the addition of localized components is more difficult to achieve.

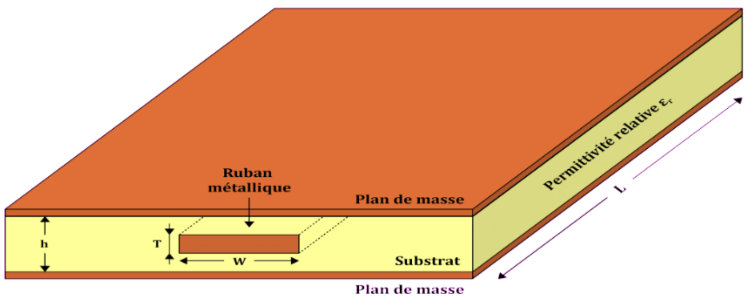

Figure I.5: Tri-plate line.

I.3 Filters

Filters are key components of modern communication systems, they allow many applications (telecommunications, instrumentation, video, radars...) to share and make the best use of the limited resource that is the spectrum, in particular by making it possible to limit the interference of the systems with respect to each other. The filters can be classified into five types: low-pass, high-pass, band-pass, band-cut and multi-band. The design of a filter is a complex engineering that requires a well-developed methodology. The design of the filters needs a new procedure and structure to obtain good simulation results. The DGS technique is one of the key solutions to achieve better performance. Like any telecommunication device in the microwave domain, the characteristics of the filters vary according to the frequency domain of operation. The usual name of the microwave bands is given in Table I.1.

I.3.1 Definition of the filter

A filter is a two-port network used to shape the frequency response of a microwave system at a given time. It allows signals within a specified passband to pass through while attenuating those outside this range, known as the stopband. Common types of frequency responses include low-pass, high-pass, band-pass, and band-stop characteristics. An ideal filter would exhibit complete attenuation in the stopband, zero insertion loss within the passband, and a linear phase response to prevent signal distortion [I.14].

Table I.1: The different telecommunications applications according to their frequency.

Band	Frequencies	Applications
L	1 to 2 GHz	Mobile communication
S	2 to 4 GHz	
C	4 to 8 GHz	Fixed service
X	8 to 12.5 GHz	Military applications
Ku	12.5 to 18 GHz	Fixed service
K	18 to 26 GHz	
Ka	26 to 40 GHz	

I.3.2 Role of The Filters

The filtering is a form of signal processing, obtained by sending the signal through an electronic circuit assembly, which modifies its frequency spectrum and / or its phase and therefore its temporal shape.

It can act either:

- To eliminate or weaken undesirable parasite frequencies

- To isolate in a complex signal, the two bands of useful frequencies.

I.3.3 Classification of filters

a- Low-pass filter: it allows the transmission of signals with low or no attenuation at frequencies lower than a predetermined critical frequency, called the cut-off frequency, and rejects the signals at frequencies higher than the cut-off frequency.

b- High-pass filter: it allows the transmission of little or no attenuated signals at frequencies higher than the cut-off frequency and signal rejections at frequencies lower than the cut-off frequency.

c- Band-pass filter: it authorizes the transmission of signals with frequencies belonging to a band limited by a lower and upper cut-off frequency and rejects the signals outside this band.

d- Band-cut filter: it rejects the signals in a frequency band limited by a lower and upper cut-off frequency and allows transmission at frequencies located outside this band.

I.3.4 Templates Filters

An ideal filter presents:

- A zero attenuation in the frequency band that it is desired to preserve (Pass-band).
- An infinite attenuation in the band that the wave wishes to eliminate (Attenuated band).

In practice, it is impossible to achieve a perfect filter. Therefore, the goal is to approximate the ideal response by:

- Maintaining attenuation below a specified maximum within the passband.
- Ensuring attenuation exceeds a specified minimum within the stopband.

This approach leads to the definition of a *template*, which outlines the acceptable and forbidden regions for the filter's frequency response curve. The filter's attenuation graph must strictly remain within these defined boundaries. Depending on the desired frequency response, four main families of filters are typically defined (see Figure I.6).

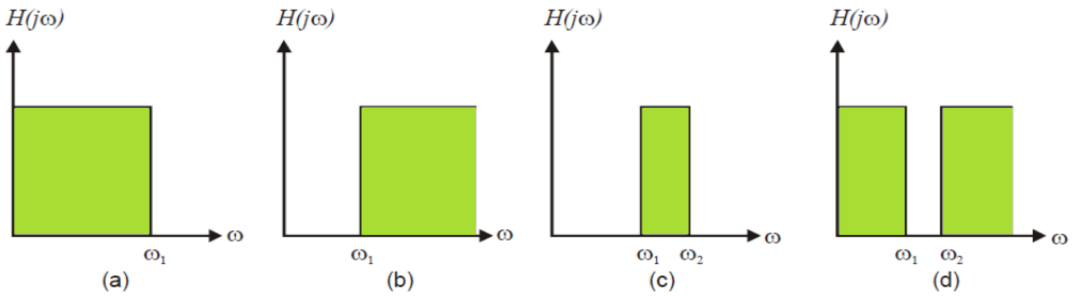

Figure I.6: Dimensions of the Ideal filters: (a) low-pass, (b) high-pass, (c) bandpass and (d) stopband [I.12].

Thus, with each filtering application, a specification is associated comprising the specifications defined by a template. The figures I.7 and I.8 illustrate the example of this template for the case of low-pass filter and the band-pass filter respectively.

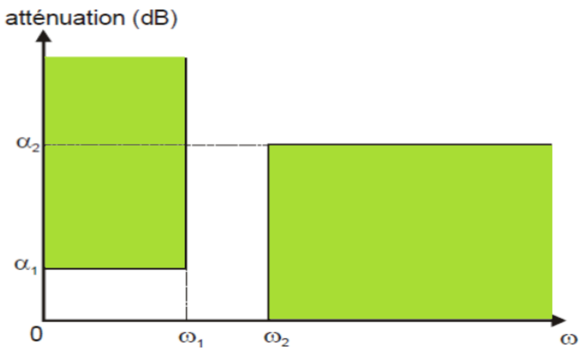

Figure I.7: Example of work books with a low-pass filter **[**I.14].

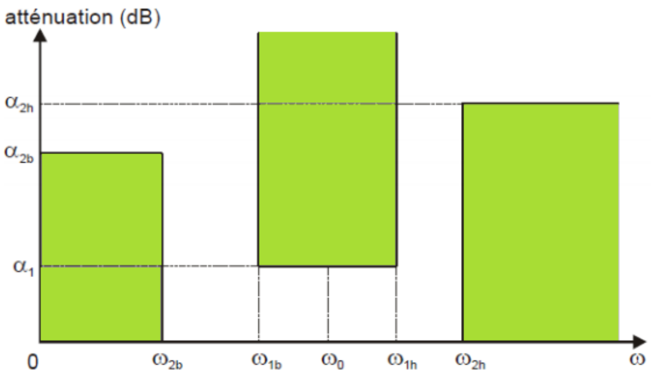

Figure I.8: Example of specifications for a bandpass filter [I.14].

I.3.5 Quadrupole matrix[S]

A filter may be represented by a Passive Quadrupole (no auxiliary electric power sources) described in Figure I.9.

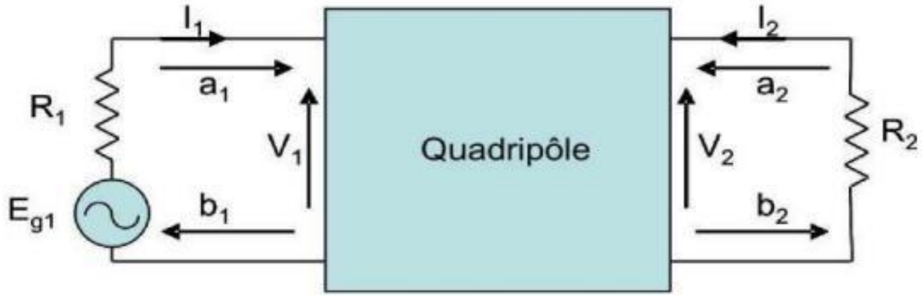

Figure I.9: Representation of the filter by a quadrupole [I.14].

V_1, V_2: Input and output voltages of the quadrupole.

I_1, I_2: Input and output current of the quadrupole.

In the field of microwaves, a quadrupole is generally defined by its parameters S_{ij} (Scattering Parameters: distribution parameters) which make it possible to completely define the characteristics of a linear multi-pole not comprising internal energy sources and in particular of a passive linear quadruple such as a passive filter. The fluency graph of the parameters S_{ij} is presented in Figure I.10 [I.14].

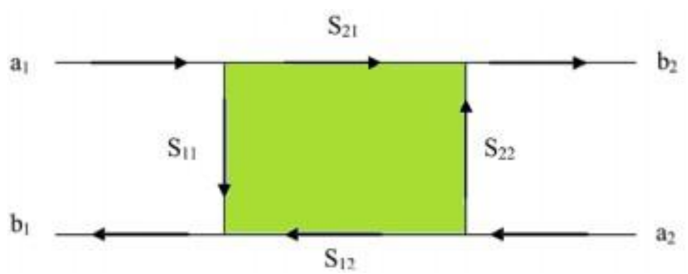

Figure I.10: Flow graph of a quadrupole.

The outgoing probes b_i are linked to the incoming ones a_i by:

$$\begin{bmatrix} b1 \\ b2 \end{bmatrix} = \begin{bmatrix} S11 & S12 \\ S21 & S22 \end{bmatrix} \begin{bmatrix} a1 \\ a2 \end{bmatrix} = [S] \begin{bmatrix} a1 \\ a2 \end{bmatrix} \quad \text{(I.34)}$$

- The coefficient S_{12} represents the coefficient of transmission at the input when the output is adapted.

- The Coefficient S_{21} represents the coefficient of the transmission to the output when the input is adapted.

- The Coefficient S_{11} represents the coefficient of input reflection when the output is adapted.

- The Coefficient S_{22} represents the reflection coefficient at the exit when the input is adapted.

A quadrupole is linear when it consists only of dipoles and linear elements. We can thus define different parameters as follows [I.14-I.16]:

The available power of the generator P_A:

$$P_A=\frac{|Eg\ 1|^2}{8R1} \tag{I.35}$$

The reflected power at the input P_1:

$$P_1=\frac{|V\ 1|^2}{2R1} \tag{I.36}$$

The power delivered to the load P_2:

$$P_2=\frac{|V2|^2}{2R2} \tag{I.37}$$

The insertion experts are defined by:

$$\frac{P_A}{P_2}=\frac{1}{|H(jw)^2|}=\frac{1}{|S21(jw)|^2} \tag{I.38}$$

The reflection experts are defined for:

$$\frac{P_A}{P_1}=\frac{1}{4\frac{|v1|^2R1}{|Eg1|^2R2}}=\frac{1}{|T(jw)^2|}=\frac{1}{|S11(jw)|^2} \tag{I.38}$$

$H(j\omega)$and$T(j\omega)$are respectively the transfer function and the reflection function of the quadruple. When the quadruple is purely reactive [I.16].

$$|H(j\omega)|^2+|T(i\omega)|^2=|S_{21}(j\omega)|^2+|S_{11}(j\omega)|^2=1 \tag{I.38}$$

I.3.6 Transfer Function Notice

The design of a filter usually begins with the determination of the transfer function that satisfies a given filter specification. Since the physical processes in electrical circuits can be represented as integrals and derivatives of currents and voltages, it is convenient to use complex variables for the analysis of circuits with harmonic excitations in the frequency domain, and the transfer function can be specified mathematically in the form of a ratio of two polynomials of complex frequency. The analytical expression of the transfer function constitutes an interface between the initial specification and a prototype of a low-pass filter whose cut-off frequency is standardized to unity. In this section, we briefly describe the types of polynomials commonly used for the approximation of the filter frequency responses [I.17].

Figure I.11 illustrates a double-terminated lossless transmission network that can represent a lossless band-pass filter.

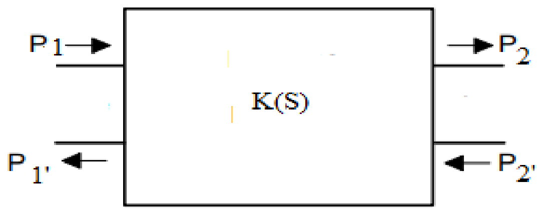

Figure I.11: Linear network without loss at double termination.

Suppose that $P1$ is the input power to be transmitted by the circuit, while $P2$ is the output power available to the load since in these Passive Dishes, $P2$ cannot exceed $P1$, it should be noted that:

$$\frac{p1}{p2} = 1 + |k(s)|^2_{s=jw} \tag{I.39}$$

Where $K(s)$ is a rational function in $s$with real efficiencies. On the other hand, the inverted power ratio of equation I.39 is a squared value of the transmission coefficient, known in the theory of the transmission line under the diffusion parameter.

$S21(s)$:

$$|s21(s)|_{s=jw}^{2} = \frac{1}{1 + |k(s)|^2_{s=jw}} \tag{I.40}$$

The reflective strength is characterized by the reflection efficiency, or parameter of broadcast

$S11(s)$, which is linked (for lossless networks) to $S21(s)$ via:

$$S11(s)|^2 + |S21(s)|^2 = 1 \tag{I.41}$$

We can show that, for the variable linear networks in the meantime, we can represent $S11(s)$ in the form of a report:

$$S(11) = (F(s))/(E(s)) \tag{I.42}$$

Thus, taking into account equation I.42, it is correct that:

$$S(21) = \frac{P(s)}{s} * (E(s)) \tag{I.43}$$

$$P(s).P(-s) = E(s).E(-s) - \varepsilon 2.F(s).F(-s) \tag{I.44}$$

The polynomials $E(s)$, $F(s)$ and $P(s)$ are called polynomials features the determination of their coefficients from the given specification raises the problem of the approximation. The function $K(s)$ is known as the characteristic function, which can be derived from the characteristic polynomials using the following expression

In Equation I.44, the ripple constant ε is introduced to normalize the maximum amplitude of the filter's passband. During the synthesis process, the polynomials are normalized so that their highest-degree coefficients are equal to one. Any resulting constant factor is then incorporated into the ripple constant.

I.4 Different Approximation Functions

In general, several characteristic functions are available for approximation. However, several classical functions are traditionally noted. These Are butter worth, Chebyshev and Chebyshev inverse, Causer or elliptic and their modifications.

Figure I.12 illustrates the low-pass prototype of three types of filters The properties and characteristics of these characteristic functions are described in the following sections.

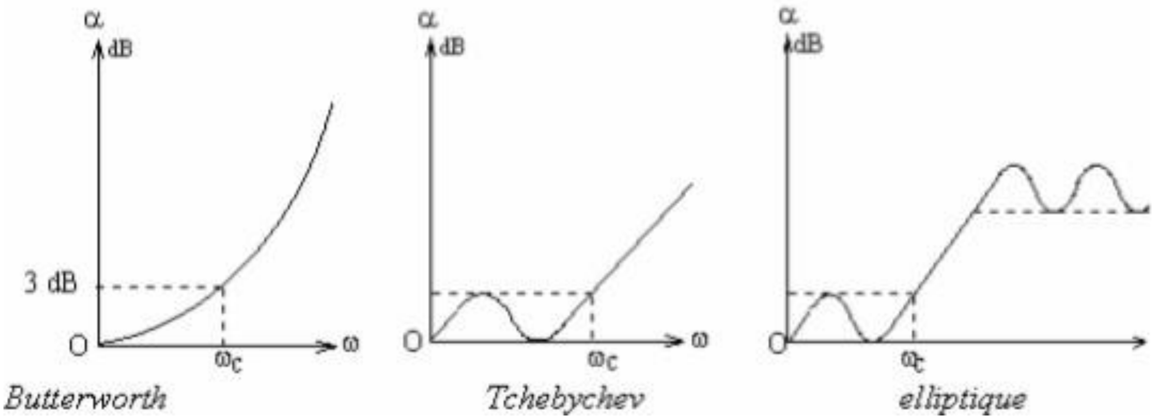

Figure I.12: Low-pass prototype of the three types of filters [I.17].

I.4.1 Butterworth Approximation

The Butterworth approximation provides the simplest approximation of an ideal prototype filter [I.6]. The Butterworth approximation is defined by:

$$K(\omega) = \omega^n \tag{I.45}$$

Where n is the order of the prototype filter, which corresponds to the number of reactive elements needed in the low-pass prototype filter. The parameters$Sij$of the filter prototype can be expressed as follows:

$$|s21(j\omega)|^2 = \frac{1}{1+\omega^{2n}} \tag{I.46}$$

$$|s21(j\omega)|^2 = \frac{\omega^{2n}}{1+\omega^{2n}} \tag{I.47}$$

Therefore, the insertion date is given by:

$$L_A(\omega) \ = 10log_{10}[1+\omega^{2n}] \tag{I.48}$$

The figure I.13 illustrates the response of a Butterworth filter for different orders

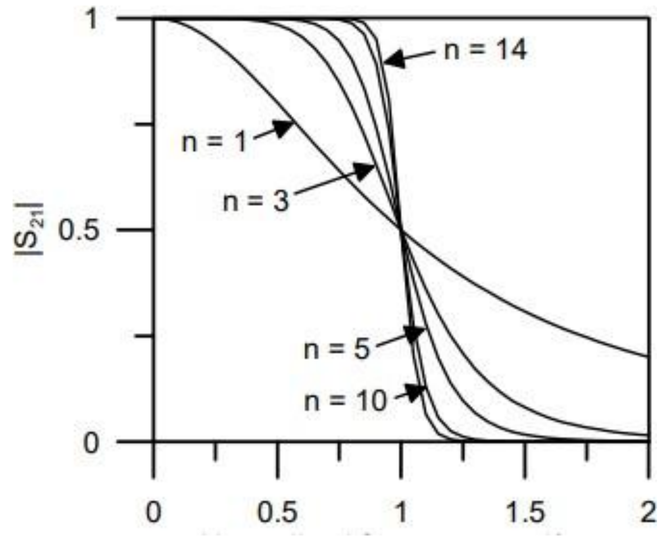

Figure I.13: Response of a filter will start with different orders [I.17].

I.4.2 Tchebychev approximation

The Tchebyshev approximation provides a sharper slope for the lower filter order n, in comparison with the flatter approximation, but introduces equal undulations in the passband [I.18, I.19]. The characteristic function of Tchebychev is defined as follows:

$$K(\omega) = \varepsilon Tn(\omega) \tag{I.49}$$

The expressions for the parameters Sij of the proto filter type are given by:

$$|s11(w)|^2 = \frac{T_n^2(w)}{1+\varepsilon^2 T_n^2(w)} \tag{I.50}$$

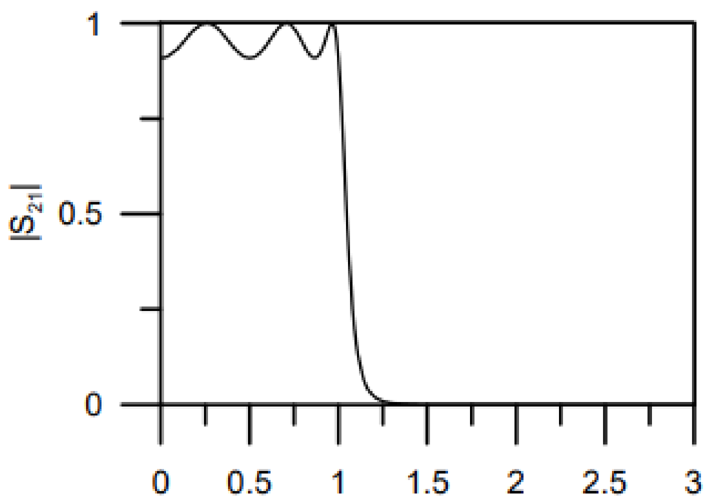

Figure I.14: Answer of a Tchebycheff filter [I.17].

I.4.3 The elliptic approximation

An elliptic approximation provides a solution with an equal ripple of the insertion loss in the pass-band and the stopped band. Due to this property, the attenuation slope is as strong as possible. The characteristic function used for this type of approximation depends on the Jacobean elliptic function$sn\ (x)$ and the complete elliptic integral of the first type K. The characteristic function can be expressed as follows:

$$k(s) = \varepsilon . s \prod_{v=1}^{(n-1)/2} \frac{(s^2 + a_{2v}^{\ 2})}{\left(s^2 a_{2v}^{\ 2} + 1\right)} \tag{I.51}$$

$$k(s) = \varepsilon \prod_{v=1}^{n1/2} \frac{(s^2 + a_{2v-1}^{\ 2})}{\left(s^2\, a_{2-1}^{\ 2} + 1\right)} \tag{I.52}$$

$$\text{When } av = \sqrt{\sin\theta}\ .sn[\frac{vK(sin\theta)}{nv}] = 1,2, \ldots, n \tag{I.53}$$

Here $sin\theta$=ωp/ωs ;ωp and ωs are the cut-off frequencies that determine the wavy intervals in the pass-band and the stop-band, respectively for a specific prototype with transmission zeros ωz1,...,ωzm and poles ωP1,...,ωPk, the transfer function can be expressed in the following form:

$$S_{21}(w)^2 = \frac{1}{1+\frac{(w^2-w^2p1)\ldots(w^2-w^2pk)}{(w^2w^2z1)-(w^2-w^2zm)}} \tag{I.54}$$

The attenuation is given by:

$$L_{Aw} = 10log_{10}[\frac{1}{1+\frac{(w^2-w^2p1)\ldots(w^2-w^2pk)}{(w^2w^2z1)-(w^2-w^2zm)}}] \tag{I.55}$$

FigureI.15 illustration of the typical response of a filter with elliptical approximation.

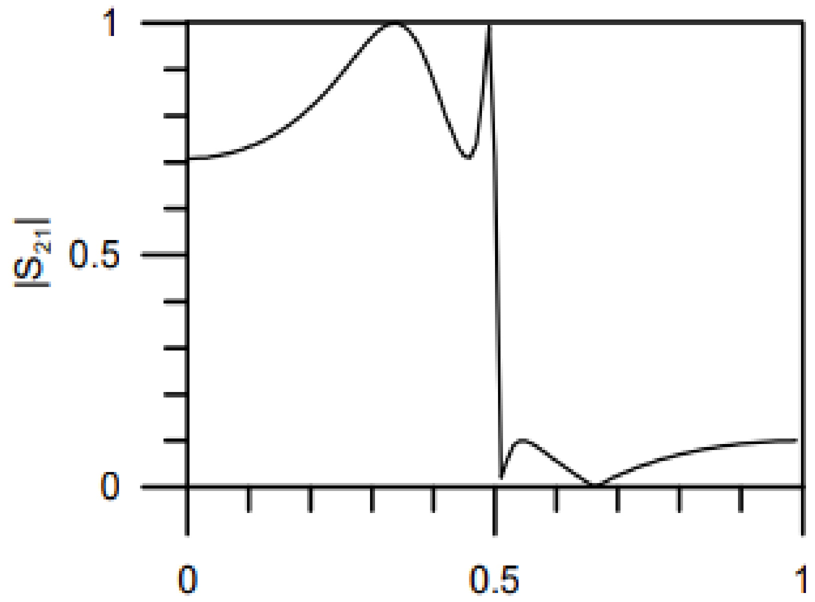

Figure I.15: Response of an elliptical filter [17].

I.5 General information about band-pass filters

A band-pass filter is distinguished because its response has a range of transmission frequencies defined as band-pass, centered at a frequency $f0$, and two attenuated bands located on each side of the pass-band. The electrical characteristics that determine its operation are the center frequency, the bandwidth, the level of rejection of the attenuated bands, the insertion losses and the flatness. These specifications are given in the electrical parameter, of which the purpose is to define the characteristics of the response that the filter must perform. In addition, the parameters that make it possible to measure the electrical performance of a band-pass filter are the level of insertion and return losses in the pass-band, the attenuation level of the rejected band and the flatness. Fig. I.16 illustrates the frequency response of a band-pass filter, its electrical template and its electrical characteristics.

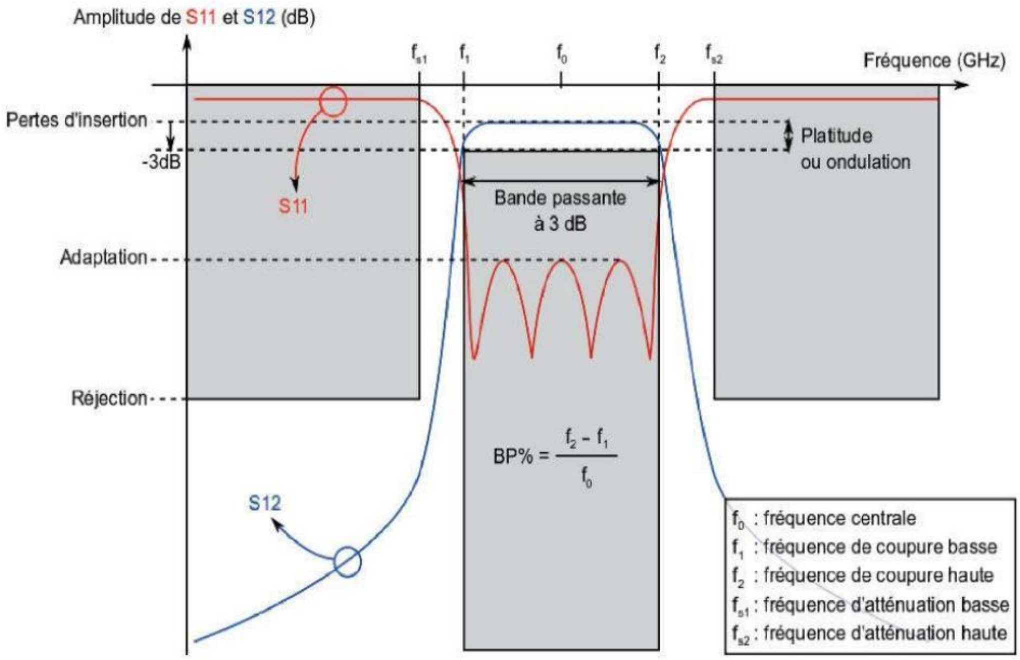

Figure I.16: Template of a band-pass filter [I.12].

I.5.1 Expressions used in the filters

➢ **Insertion loss**

The insertion step is defined as the attenuation level of the parameter S_{12} measured at the center frequency $f0$, that is to say on the electrical response during transmission. The importance of this parameter lies in the fact that it encompasses all the sources of losses encountered inside the resonant element as well as the losses due to the interactions between the coupling structures of the resonator with the outside (radiation losses, dielectric, ohmic, metallic, etc.).

During the adjustment process of a microwave filter, its adaptation level must be set to be better than -15 dB at f_0, in order to ensure that the attenuation value corresponds to an insertion loss level value and not to a mismatch of the response

➢ **Loss of return**

It is the ratio between the power returned by a tested device, by a discontinuity in a transmission line or an optical fiber, and the power injected into this device, generally expressed as a negative number in dB. This discontinuity may be a mismatch with the terminal load or with a device inserted in the line.

- **Bandwidth**

For a bandpass filter, this is the difference between the upper and lower frequencies generally recorded at attenuation points of 3 dB above the passband.

- **Cut-off frequency**

The cut-off frequency is the frequency at which the insertion loss of the filter is equal to 3 dB

- **Stop band**

The stop band is equal to the frequency range in which the filter insertion loss is greater than a specified value. This is the out-of-bandwidth group.

- **Ripple**

The flatness of the signal in the bandwidth can be quantified by specifying the ripple or the difference between the maximum and minimum amplitude response in dB.

- **Rejection**

For an ideal filter, we would obtain an infinite attenuation level for the unwanted frequencies of the signal. However, in reality we are expecting at an upper limit due to the deployment of a finite number of filter components. Practical designs often specify 60 dB as the rejection rate.

I.5.2 Quality factor

The quality factor of a filter is consolidated as an important parameter that defines the degree of quality of such a device [I.20]. The quality of a filter depends on the quality of its resonators, whose structure is generally identical or very similar. There are three types of quality factors, the unloaded quality factor QU, the loaded quality factor QL and the external quality factor QE. They are described as follows:

Charged quality factor: The charged quality factor QL is a dimensionless quantity that measures the selectivity of a charged resonator at its resonant frequency, that is to say when the resonator is coupled to an external circuit impedance. It is determined using the following equation, using the answer of the parameter S_{21}:

$$Ql = \frac{f0}{BW3\text{db}} = \frac{f0}{f2-f1} \qquad \text{(I.56)}$$

Here, $f0$ is the resonance frequency and $BW3dB = f2 - f1$ corresponds to the passband calculated at -3 dB from the insertion losses perceived under resonance conditions, as we can see at Figure I.17 according to the equation (I.56), the valor of selective is incremented as the filter becomes more.

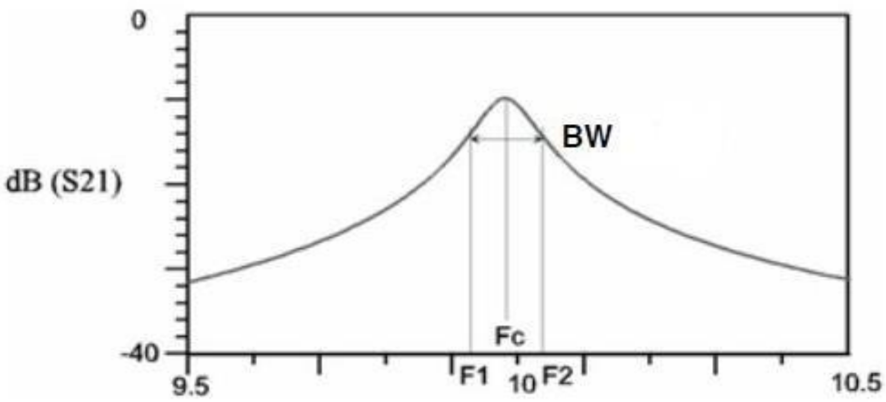

Figure I.17: The passing band has -3dB [I.12].

External quality factor: The external quality factor characterizes the losses produced by the external coupling structures of the resonator. It is defined by the following equation [I.20, I.21]:

$$Q_E = W_0 \frac{stored\ risonator\ per\ cycle}{power\ dissipated\ by\ the\ external\ load\ per\ cycle} \quad \text{(I.57)}$$

$$\text{When: } w_0 = 2\pi f_0 \quad \text{(I.58)}$$

Equation I.58 corresponds to the pulse measured at the resonance frequency. A common dual-load resonator has two associated external quality factors, one related to input losses and the other related to output.

Moreover, the external quality factor can also be expressed by:

$$Ql = \frac{f0}{BW3\text{db}} = \frac{f0}{f2-f1} \quad \text{(I.59)}$$

$$Q_E = \frac{Q_l}{S_{21}f_0} \quad \text{(I.60)}$$

Here, QL corresponds to the loaded quality factor and $S_{21}f_0$ is the natural value of the parameter S_{21} Measured under resonance conditions. The value of could also be characterized experimentally by means of the phase method proposed in [I.22]. This method is based on the calculation of the ratio between the resonance frequency $f0$ and the bandwidth Δf which corresponds to a phase shift of ± 90° of the reflection coefficients. Then the value of QE can be expressed by:

$$QE = \frac{f_0}{|\Delta f \neq 90°|} \tag{I.61}$$

Unloaded Quality Factor

The unloaded quality Factor evaluates the intrinsic electrical performances of a resonator when it is not coupled to any

External circuit Theoretically, the unloaded quality factor is defined by the equation:

$$QE = W0 \; \frac{\text{stored risonator par cycle}}{\text{power dissipated by the external load per cycle}} \tag{I.62}$$

The previous expression theoretically explains the concept of an unloaded quality factor; however, its practical use is difficult. A more useful expression for evaluating it by measurements is given by Equation I.63. It connects the loaded quality factor values $QL$with the unloaded quality factor $QU$and the external quality factor QE.

$$QE = W0 \; \frac{\text{stored risonator par cycle}}{\text{power dissipated by the external load per cycle}} \tag{I.63}$$

The value of the factor of equality not charged can be derived.

$$Q_U = \frac{Q_L}{1 - |S_{21} f_0|} \tag{I.64}$$

I.6 Filtering by DGS filter

I.6.1 Defected Ground Structures (DGS)

In recent years, a new and different concept has been applied for the distribution of microwave circuits. One of these techniques is the defective ground structure or DGS, where the ground plane of a micro strip circuit is intentionally modified to improve performance. The name of this technique simply means that a "fault" has been placed in the ground plane, which is generally considered an approximation of a perfectly conductive infinite current collector. Indeed, a microwave ground plane is far from the ideal behavior of a perfect earth. Although the additional disturbances of the DGS modify the uniformity of the ground plane, they do not make it defective [I.23].

The defective ground structure (DGS), engraved in the ground plane of a plane printed circuit board, constitutes a promising approach to increase the reduction of the stop band and reduce the size of the passive components [I.24].

I.6.2 DGS as periodic structures

Since 2001, many researchers have been tempted to use periodic deceleration resolution systems to improve the performance of amplifiers, power monitors, oscillators and filters. So, they suggested using a micro-strip line with periodic DGS at the output for the harmonic an adjustment of different components.

I.6.3 Different forms of DGS

There are different forms of DGS structures used for the design of compact and high-performance microwave components, such as: rectangular, square, circular, dumbbell, spiral,

L-shaped, concentric ring, U-shaped and V-shaped, pin DGS, hexagonal DGS, cross-shaped DGS [I.14] (Figure II.13). Each DGS form can be represented in the form of a circuit consisting of an inductor and a capacity, which can lead to a certain frequency band interval determined by the shape, dimension and position of the defect.

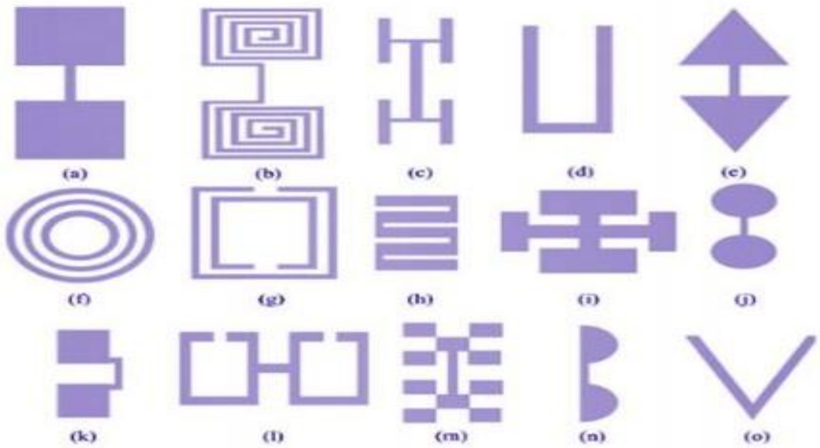

Figure I.18: Different types of DGS [I.14].

I.6.4 The characteristics of the elements of the DGS

- **DGS Advantages**

The most important features of the DGS are: improve the performance of the stop-band, disturbance of the shielding fields on the ground plane, and easier to model and so to use in more complex structures.

- **Disadvantages of DGS**

Radiation in closed microwave circuits can be difficult to include in the simulation.

I.6.5 Equivalent DGS circuit

A parallel LC circuit (see Figure I.19) can represent the equivalent circuit of the DGS, as indicated from his answer. From the point of view of the application, the DGS section can replace a parallel LC resonator circuit in many applications. The equivalent LC circuit of DGS can be extracted be case this type of electrical characteristic is observed from a typical LC parallel resonant circuit.

$$jXlc = \frac{jwlp \times \frac{1}{jwCp}}{jwlp + \frac{1}{jwCp}} = \frac{jwLp}{1 - w^2LpCp} \quad \text{(I.65)}$$

$$w^2 = \frac{1}{LpCp} \quad \text{(I.66)}$$

$$Xlc = \frac{1}{w0c(\frac{w0}{w} - \frac{w}{w0})} \quad \text{(I.67)}$$

$$Xl = w'Z0g1 \quad \text{(I.68)}$$

It is shown that the DGS is equivalent to a simple parallel resonance circuit, as indicated in Figure I.19, where the equivalent inductance and the equivalent capacitance are given by the following equations:

$$Cp = \frac{5fc}{\pi(f_0^2 - f_c^2)} \quad \text{(I.69)}$$

$$Lp = \frac{1}{w_0^2} \quad \text{(I.70)}$$

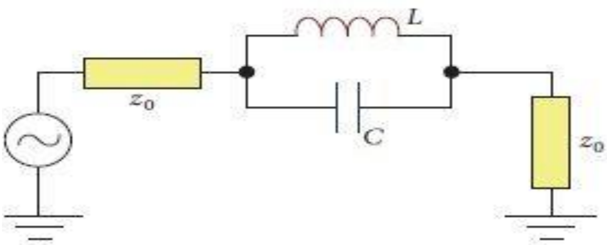

Figure I.19: equivalent circuit [I.12].

I.7 Different types of micro wave filters

I.7.1 Band-pass filter topologies

In the literature, an appreciable number of filter topologies having pass-band characteristics have been reported. They could be classified into two categories according to their bandwidth. Medium and wide band filters, the fractional bandwidth of which is between 20 and 80%, and narrow band filters, which have a fractional bandwidth of less than 20%. A brief description of the topologies belonging to each group is presented below.

I.7.1.1 Medium and wide band filters

This category includes filters whose FB is between 20 and 80%. This type of filters is mainly used in telecommunications and radar applications for working with high data rates. The classic topology to meet these requirements is the metal filter, integrated into the short-circuit leads λg/4 or to short-circuit leads of λg/2 [I.27, I.28].

I.7.1.2 Topology of stubs filters

The coupling filter is composed of long shunt connections of $\lambda g0/4$ for the short-circuited tuning filter and $\lambda g0/2$ for the open-circuit coupling filter, connected by long-inlet inverters of$\lambda g0/4$, where $\lambda g0$ is the guided wavelength in the propagation medium at the center frequency $f0$. The synthesis procedure involves the calculation of the characteristic admittances of the two connection lines and the admittance inverters taking into account the given specification, then their respective dimensions [I.24, I.26].

The short-circuit filter is known to have its second pass-band centered on $3f0$ and an attenuation pole located on $2f0$. On the other hand, the closed-circuit filter with an open circuit will have attenuation poles whose location depends on the synthesis parameters and additional pass-bands centered in the vicinity of 0 and $2f0$ and at other periodic frequencies [I.26]. If this filter is used for a narrowband specification, the synthesis produces low impedance stubs which pose problems of feasibility and electrical performance. Fig. II.15 shows the basic diagram of a short-circuit connection filter and an open circuit.

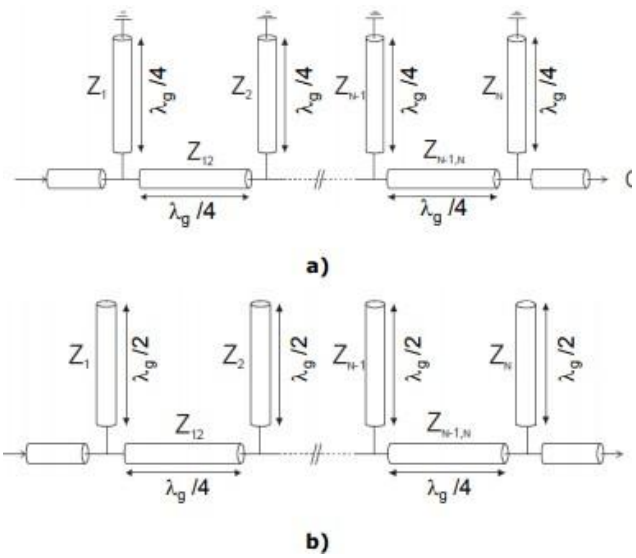

Figure I.20: Diagram of a stub filter: a) Short-circuited stub filter; b) Open stub filter I. [12].

I.7.2 The waveguide technology

Waveguide technology was the basis for the first reported microwave filters and continues to play a key role in the design of communication systems, especially for satellite payloads. They are characterized by their high-power processing capacity and their low losses due to their high Qu values (Qu> 10,000), which allows the synthesis of filter functions with very selective responses (FBW of 2% or less). Despite its excellent performances, their weight and their bulk are well-known disadvantages of this technology [I.24, I.26]. For these reasons, they occupy an important place in the payload and therefore contribute significantly to the selling price of the satellite [I.27].

Waveguide filters can be classified into three categories: cavity filters, waveguide filters, and dielectric resonator filters, the characteristics of which are described below.

I.7.2.1 Cavity filters

Cavity filters are composed of metal cavities built inside a block of metal. Their inter-resonator couplings are carried out thanks to the use of openings etched in the walls of the cavity. Theoretical equations for determining the dimensions of the cavities and an abacus calculation for calculating the coupling structures between the filter elements are available in [I.24]. Bi-mode cavities with two orthogonal polarizations at the same frequency could be used to reduce the filter footprint. Then, filters of order $2N$ can be created with resonators.

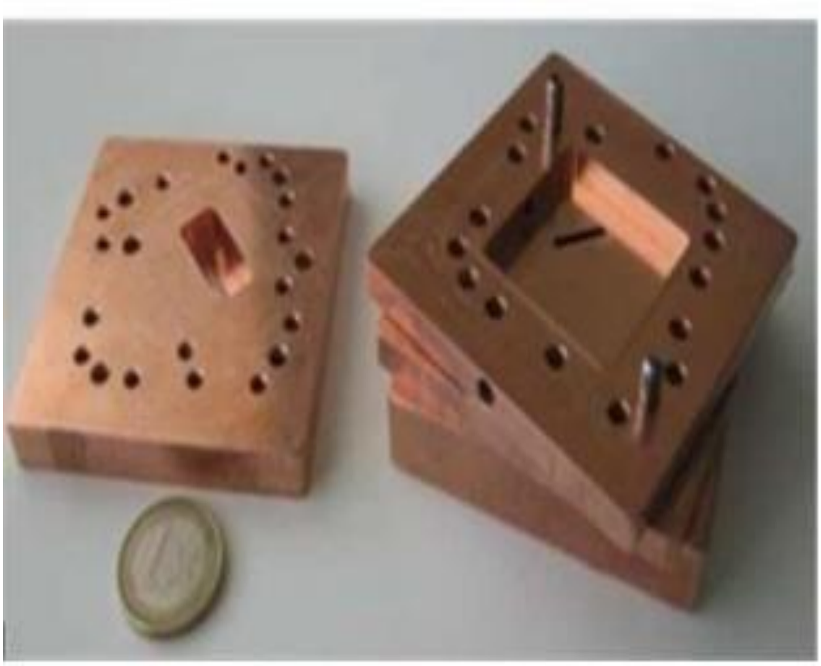

Figure I.21: Cavity filters [I.12].

A discontinuity of 45° with respect to the excitation axis, generally achieved using screws or adjustment slots, is introduced to couple the double polarizations mode [I.12].

I.7.2.2 Waveguide filters

Waveguide filters are composed of a traditional waveguide in which certain metal plates are positioned so as to form a series of cavities coupled by irises. The nature of the coupling (electrical or magnetic) is determined by the position of these coupling structures. The design equations of this filtering technology are well known and documented [I.26, I.28]. An example of a rectangular waveguide filter is illustrated in Figure I.22.

The level of losses of the technology is reduced due to the absence of a dielectric and the use of high-conductivity metallization in the boundary walls. For this reason, they are used in high-frequency applications, such as RF front-end chains and satellite transmission chains, which require low loss, high selectivity and a high diversity of free-band parasites [I.30]. The disadvantages of the technology lie in its large associated foot print, due to the reduced value of εr and the difficulty in developing complex filtering functions when particular modes are used.

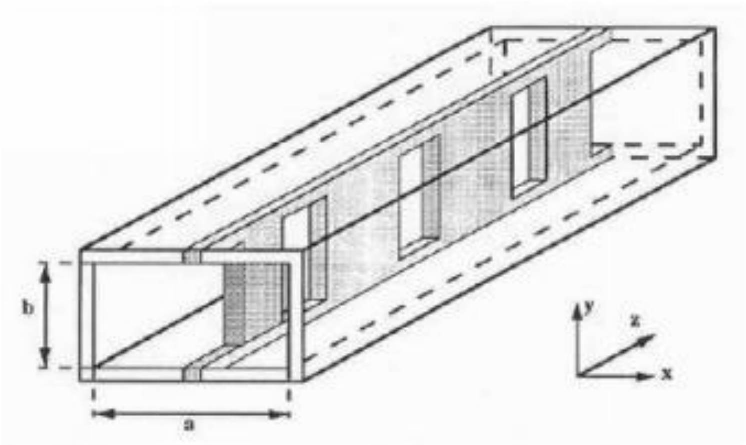

Figure I.22: Waveguide filters [I.12].

I.7.2.3 Dielectric resonator filters

Dielectric resonator filters are composed of high permittivity dielectric blocks of circular or rectangular geometric shapes and magnetic walls resulting from the difference in permittivity between the dielectric and the air. The inter-resonator couplings are carried out in air and the inlet/outlet couplings are carried out using micro-ribbon lines or a coaxial cable. Due to the use of high permittivity dielectrics, these filters are less bulky than metal cavity filters, which makes it possible to obtain high Qu values [I.24]. Figure I.23 shows a filter developed in [I.31] based on this technology which uses dual-mode resonators in order to reduce the total size of the structure.

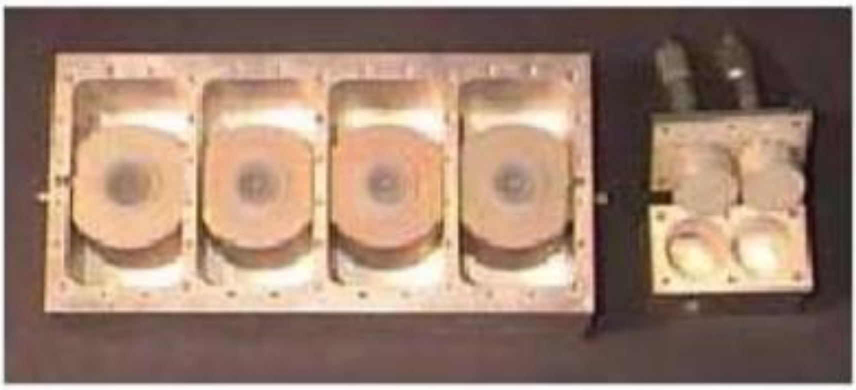

Figure I.23: Dielectric resonator filters [I.12].

I.7.2.4 Substrate Integrated Waveguide (SIW)

SIW is a technique which consists of the integration of a rectangular waveguide in a microstrip substrate, which makes it possible to group it as a planar technology. This technique, developed by D. Deslandeset K. Wu [I.32], makes it possible to draw from a higher factor Qu provided by the propagation modes of the waveguide, combined with the versatility and compactness of the plane lines, thus offering low loss responses and high-power management.

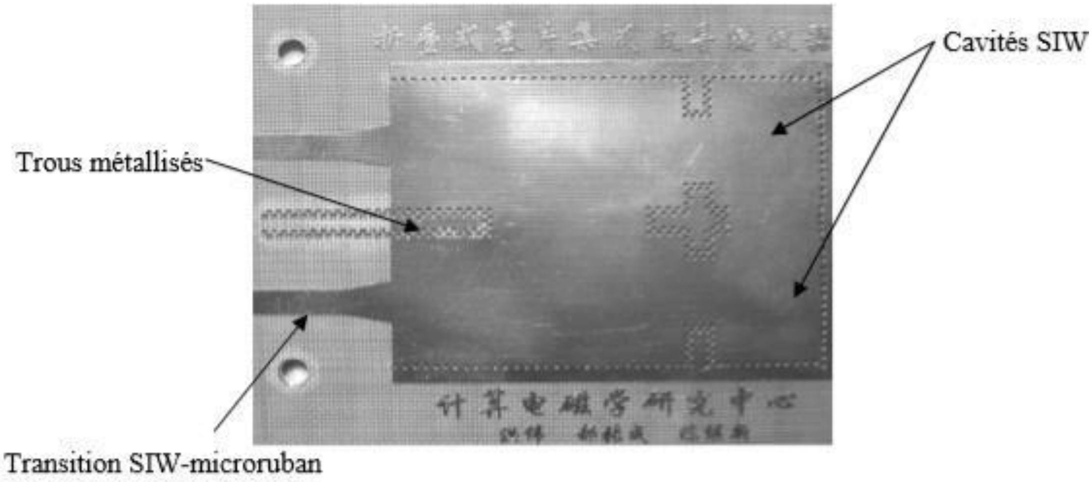

Figure I.24: Filter SIW [I.33].

I.8 Conclusion

This chapter has presented a comprehensive overview of the theoretical foundations and technological advancements underpinning modern microwave filter design. Beginning with an exploration of the fundamental principles of electromagnetic wave propagation in rectangular and planar waveguides, we have established the essential groundwork for understanding how different transmission line structures influence filter behavior. Particular emphasis was placed on planar technologies—such as microstrip, coplanar, and tri-plate lines—highlighting their role in reducing cost, size, and complexity in practical applications. The study then shifted focus to filter design principles, classifications, and approximation methods, including Butterworth, Chebyshev, and elliptic functions, each offering different trade-offs between pass-band flatness and stop band attenuation. Key performance metrics such as insertion loss, return loss, quality factors, and bandwidth were discussed, providing insight into the criteria used to evaluate filter efficacy. Finally, advanced techniques like the Substrate Integrated Waveguide (SIW) and Defected Ground Structure (DGS) were introduced as innovative approaches that bridge the gap between high-performance waveguide filters and the compactness of planar circuits. These hybrid technologies not only enhance filter performance in terms of quality factor and miniaturization but also pave the way for novel, application-specific filter topologies suitable for high-frequency and space-constrained environments. Together, these developments form a solid foundation for the subsequent design and realization of complex, high-efficiency microwave filters using SIW-DGS techniques in multi-band and millimeter-wave applications.

References

[I.1] **M. A. Rabah, M. Abri, H. A . Badaoui, J. Tao, T-H. Vuong.** (2016, February). Compact miniaturized half-mode waveguide/high pass-filter design based on SIW technologyscreens transmit-IEEE C-band signals. Microwave and Optical Technology Letters.Volume.58, Issue. 2, pp. 414–418.

[I.2] **M.Casaletti, G.Valerio, R.Sauleau, M.Albani.** (2016). Mode-MatchingAnalysis of Lossy SIW Devices . IEEE Transactions on MicrowaveTheory and Techniques. Issue. 99

[I.3] **T.R.Jones, M.Daneshmand. (**2016).The Characterization of a RidgedHalf-Mode Substrate Integrated Waveguide and Its Application in Coupler Design.IEEE Transactions on Microwave Theory and Techniques. Issue. 99.

[I.4] **O.Konc, D.Maassen , F.Rautschke , G.Boeck,** ’’Wide band Substrate Integrated Waveguide Ku-Band Coupler,’’ 21st International Conference on Microwave, Radar and Wireless Communications (MIKON), 2016.

[I.5] **Z.liu, Studentmember, l.zhu and Gaobiaoxiao.** (2016,JULY).a novel micro wave attenuator on multilayered substrate integrated waveguide. IEEE transactions on components, packaging and manufacturing technology. VOL. 6, NO. 7.

[I.6] **D.Jia, Q.Feng, Q. Xiang, K.Wu.** (2016). Multilayer Substrate Integrated Waveguide (SIW) Filters With Higher-Order Mode Suppression. IEEE Microwave and Wireless Components Letters. Vol. 26, Issue: 9, pp. 678 – 680.

[I.7] **K.Zhou, W.Kang, W.Wu.** (2016). Compact dual-band balanced band pass filter based on double-layer SIW structure Electronics Letters. Vol. 52, Issue: 18, pp. 1537 – 1539.

[I.8] **F.Benzarga** ‘’ étude et conception des réseaux d’antennes a ouverture progressive pour l’imagerie passive et la technologie SIW Modélisation par la méthode des éléments finis 2D,’’Ph.D dissertation. Faculté de technologie, université de Tlemcen, 2016.

[I.9] **J.Quinet** ‘’ Théorie et pratique électronique et amplificateur. Ligne. Electrique. eq de Mawelle,’’ édition Dunod, collection science sup. 2006.

[I.10] **B. Amana et J.L. Lemaire,** ‘’Propagationd Ondes EM dans un guide à section rectangulaire,’’ Licence de Physique - Univ. de Cergy-Pontoise.2014..

[I.11] **E.PucciGap** ‘’Waveguide Technology for Millimeter Wave Applications and Integration with Antennas,’’Ph.D dissertation. Dept of Signals and Systems Chalmers, University of Technology G¨oteborg, Sweden,2013. Page 85 Bibliographie

[I.12**] J. Garreau** ‘’Étude de filtres hyperfréquence SIW et hybride-planaire SIW en technologie LTCC,’’Ph.D dissertation, Université de Bretagne occidentale - Brest, 2012.

[I.13] **S. Didouh, M. Abri, H. A. Badaoui.** (2015,December). A new C and Ku-band logarithmically periodic linear bowtie antennas array design using lumped-element equivalent schematic model AEU - International Journal of Electronics and Communications, Vol. 69, pp. 1766-1772.

[I.14] **M. A. Rabah, M. Abri, H.A Badaoui, J. Tao, and T.H.** (2016). Vuong Compact Miniaturized Half-Mode Waveguide/High Pass-Filter Design Based on SIW Technology Screens Transmit-IEEE C-Band signals. Microwave Opt Technol Lett. 58:414–418.

[I.15] **K.Dong, J.Mo, Y.He, Z.Ma, X.Yang.** (2016, October).design of a millimeter-wave wideband band pass filter with novel-slotted substrate integrated waveguide. Microwave and optical technology letters.Vol. 58, No. 10.

[I.16] **M.reza, F.Ehsan, Z.Jahromi, R.Basiri**. (2018, August). A compact semi-open wideband SIW horn antenna for K/Ku band applications. AEU - International Journal of Electronics and Communications.Vol.92, pp. 15-20.

[I.17] **T.Agrawal, Shweta, Srivastava, Ku.** (2018,April). band pattern reconfigurable substrate integrated waveguide leaky wave horn antenna. AEU - International Journal of Electronics and Communications, 87, pp. 70-75.

[I.18] **S. Doucha, M. Abri,** ‘’ A Leaky Wave Antenna Based on SIW Technology for Ka Band Applications,’’ International Conference on Electrical Engineering and Control Applications, Springer: Recent Advances in Electrical Engineering and Control Applications, vol. 411, pp. 297-305, 2016.

[I.19] **B. Fellah, M. Abri.** (2016). Design of Antipodal Linearly Tapered Slot Antennas (ALTSA) Arrays in SIW Technology for UWB Imaging. Springer: Recent Advances in Electrical Engineering and Control Applications. vol. 411, pp. 381-389.

[I.20] **R. Arora, S. B. Rana, S. Arya.** (2018, September). Performance analysis of Wi-Fi shaped SIW antennas. AEU - International Journal of Electronics and Communications. Vol. 94, pp. 168-178.

[I.21] **S. Moitra, P. Sarathee, Bhowmik.** (2016, December).Modelling and analysis of Substrate Integrated Waveguide (SIW) and half-mode SIW (HMSIW) band-pass filter using reactive longitudinal periodic structures.AEU - International Journal of Electronics and Communications.Vol. 70, pp. 1593-1600. Page 86 Bibliographie

[I.22] **M.Bozzi, A.Georgiadis, K.Wu**. (2011, June, 6). Review of substrate-integrated waveguide circuits and antennas. Microwaves, Antennas & Propagation IET. vol.5, no.8, pp.909, 920.

[I.23] **A. Suntives, R. Abhari.** (2007). Transition Structures for 3-D Integration of Substrate

Integrated Waveguide Interconnects. Microwave and Wireless Components Letter IEEE. Vol.17, No. 10, pp.697-699.

[I.24] **D. Deslandes and K. Wu.** (2001).Integrated Micro strip and Rectangular Waveguide in Planar. Microwave and Wireless Components Letters IEEE.pp.68- 70.

[I.25] **Z. Li, K. Wu.** (2008,Feb).24-GHz Frequency-Modulation Continuous-Wave Radar FrontEnd System-on Substrate. IEEE Trans. Microw. Theory Tech., vol. 56, no. 2.

[I.26] **N. A.Smith.** ‘’Substrate Integrated Waveguide Circuits and Systems,’’Ph.d dissertation, Dept of Electrical & Computer Engineering McGill, University Montréal, Québec, Canada,2010.

[I.27] **D. Deslandes and K.Wu.** (2006, Jun). accurate Modeling wave Mechansms, and design consdiration of substrat waveguide. IEEE Transaction on microwave theory and techniques.vol54, no 6.

[I.28] **M. Ando, J. Hirokawa and Al.** (1997). Novel single-layer waveguides for high-efficiency millimeter-wave arrays. IEEE millimeter waves conference proceedings, pp.177180.

[I.29] **Y. Cassivi, L. Perregrini, P. Arcioni, M. Bressan, K. Wu, and G. Conciauro.** (2002). Dispersion characteristics of substrate integrated rectangular waveguide. IEEE Microwave and Wireless Components Letters. No. 12, pp.333-335.

[I.30] **Y. Cassivi, L. Perregrini, P. Arcioni, M. Bressan, K. Wu, and G. Conciauro.** (2002, September). Dispersion characteristics of substrate integrated rectangular waveguide IEEE Microwave Wireless Compon. Lett. vol. 12, pp. 333–335.

[I.31] **D. Deslandes and W. Ke, Accurate.** (2006). modelling, wave mechanisms, and design considerations of a substrate integrated waveguide. IEEE Transactions on Microwave Theory and Techniques. vol. 54, pp. 2516-2526.

[I.32] **J. E. Rayas-Sanchez and V. Gutierrez-Ayala**. (2008,Jun). A general EM-Based design procedure for single-layer substrate integrated waveguide interconnects with microstrip Transitions. IEEE MTT-S Int. Microwave Symp. Dig., Atlanta, GA, pp. 983-986.

CHAPTER II

SIW and HMSIW techniques

II.1. Introduction

In recent years, the development of the field of telecommunications has prompted the realization of increasingly compact equipment and efficient, operating at higher and higher frequencies. The implementation practice of these devices is very expensive, since the weight and volume are parameters crucial. The waveguides are slides that have benefited the most from this development [II.1].

In the first part, we present the SIW technology. We start with the definition and advantages of the SIW guide technology then by the design rules of SIW guide and finally we finish with the transition from the micro ribbon lines to the SIW.

In the second part, we present the technique called half-mode SIW (HMSIW) which is widely used for the design of various miniaturized components intended for microwave systems, such as: antennas, filters...

II.2. Definition of substrate-integrated waveguides

The waveguides integrated into the substrate (SIW) are guides rectangular waves formed by two solid conductive planes, separated by a substrate dielectric, with conductor sidewalls emulated by rows of vias through metallized. Alternatively, the side walls of the SIW can be formed in spraying copper on laser-cut hollows in the substrate [II.2]. The side wall of via is a 1-dimensional (1-D) periodic structure that can be decomposed into a serial connection of unit cells to facilitate analysis. The SIW structure is designed by choosing appropriately spaced vias, of the same diameter, in order to support sufficiently guided wave propagation with minimal radiation losses. The spacing between the vias controls the amount of field leakage out of the waveguide. If the vias are too far apart from each other, the insulation property of the SIW will be compromised. This leakage potential sets the limit as to the possible propagation modes in this guide periodic waveform [II.3].

II.3. SIW Structure

SIW (Substrate Integrated Waveguide) structures based on rectangular waveguides are designed using two rows of metallic vias that connect the top and bottom ground planes of the dielectric substrate [II.4].

In addition to the dimensions of the metallic cylindrical vias, a new width is introduced for the SIW guide. This width refers to the distance between the two rows of vias, measured from center to center of the metallic cylinders, as illustrated in Figure II.1 below. Thus, the structure is characterized by the following dimensions:

- **d**: the diameter of a via.
- **P**: the center-to-center spacing between adjacent vias (pitch).
- $\mathbf{a_s}$, $\mathbf{a}_{siw}$: the width between two rows of vias from center to center.
- In addition to the $\mathbf{a}_{siw}$ which is the width of the equivalent rectangular waveguide, and h the thickness of the substrate. [II.5]

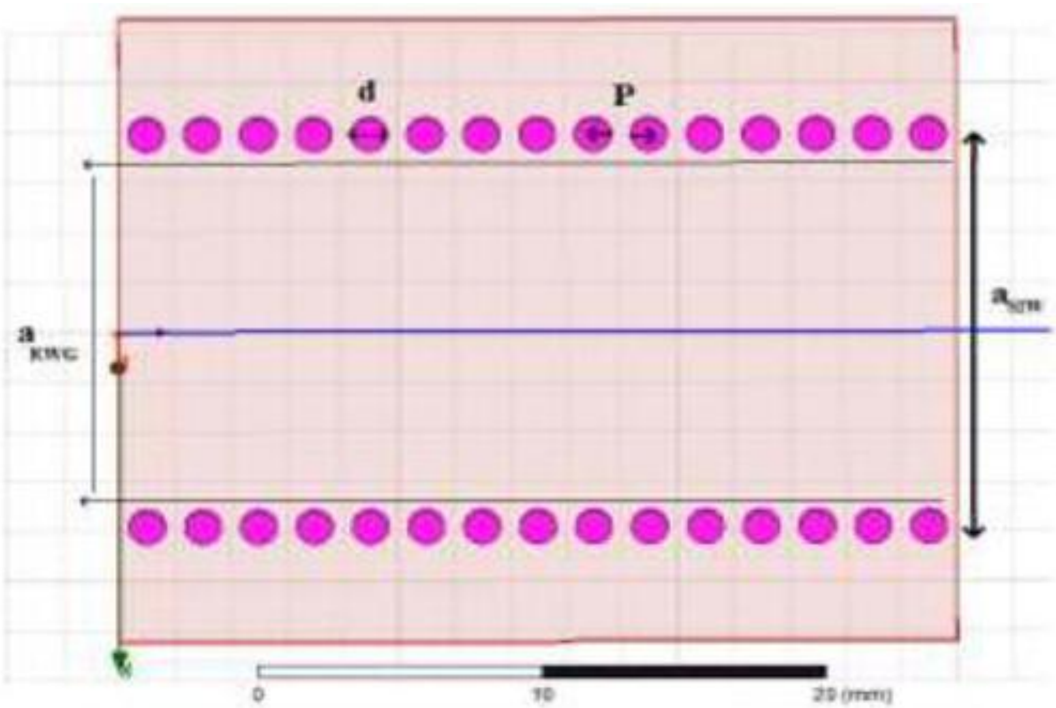

Figure II.1: Geometry of a SIW structure.

II.4. Types of SIW Structures

Just as a rectangular waveguide has parameters that characterize it, the Substrate Integrated Waveguide (SIW) also has its own inherent parameters. These include a cutoff frequency, a fundamental mode, TE impedance, an attenuation factor, phase velocity, group velocity, and so on.

To achieve better waveguide performance, the SIW is typically designed to operate at frequencies between the TE_{10} and TE_{20} mode frequencies. Various topologies have been proposed to enhance the SIW structure in terms of size and bandwidth.

One such proposed topology is the folded SIW structure, introduced in [II.6]. It involves adding a third metallic plane between the top and bottom metal layers, which touches only a single row of via holes. This modification enables a significant reduction in the overall size of the structure but comes at the cost of increased losses, as shown in [II.7].

To address this trade-off, the concept of the Half-Mode SIW (HMSIW) was introduced, in which the waveguide size is effectively halved. Figures (II-2) (a and b) illustrate these respective structures.

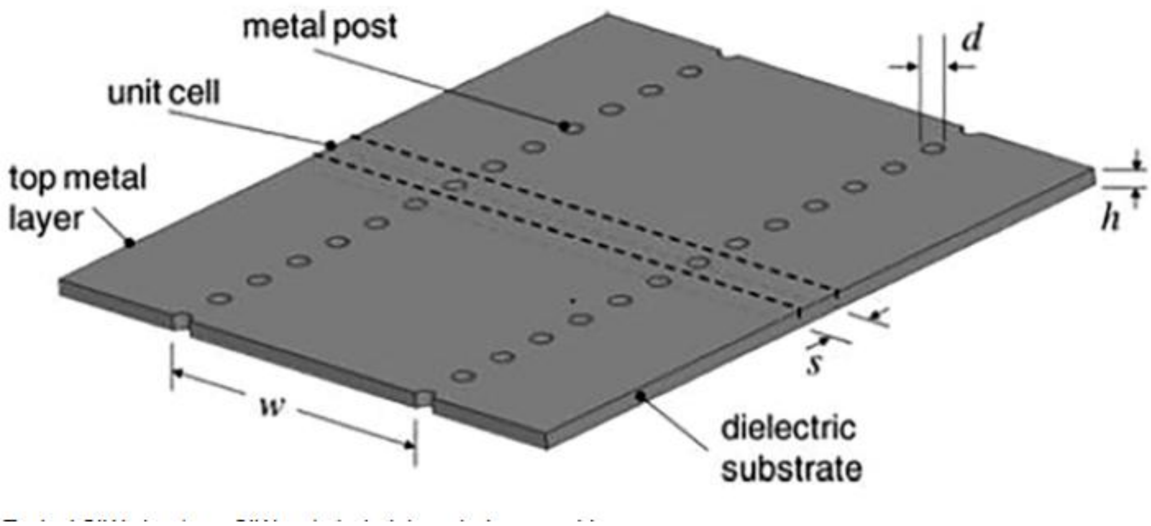

Figure II.2: Structure type SIW.

II.5. The advantages of SIW technology

The waveguides integrated into the substrate have advantages such as [II.8]:

- Low realization costs.
- Low losses.
- A high-quality factor.
- Reduced size.
- Ease of integration with other systems.

II.6. The rules of design

To design a good SIW structure it is necessary to follow a few design steps. The production of a SIW guide as illustrated in Figure II.3 is based on a substrate dielectric, which contains metal vias welded to the two conductive layers upper and lower in order to confine the electric field in the waveguide. The quantities d and s represent respectively the diameter of the metal vias and the distance between the vias.

The first step in the construction of a SIW structure is the location of the vias metallic as indicated in [II.9]. So as not to have an overlap between the vias metal the distance s must be greater than the diameter of the vias d and since the vias metal vias play the role of a metal wall, so the vias must be as close as possible However, the circuit then becomes very fragile to mechanical breakages when these vias are too close to each other, if, conversely, they are too spaced apart, the radiation losses can quickly become too high. The diameter d also has an impact on losses and must be optimized by s. It is shown in [II.10] that the ratio s/d has a direct relation on the losses and it should be used as a design parameter of a SIW guide. According to Deslandes [II.11], if $s = 2 \times d$, we can say that the radiation losses are then negligible compared to other losses [II.12]:

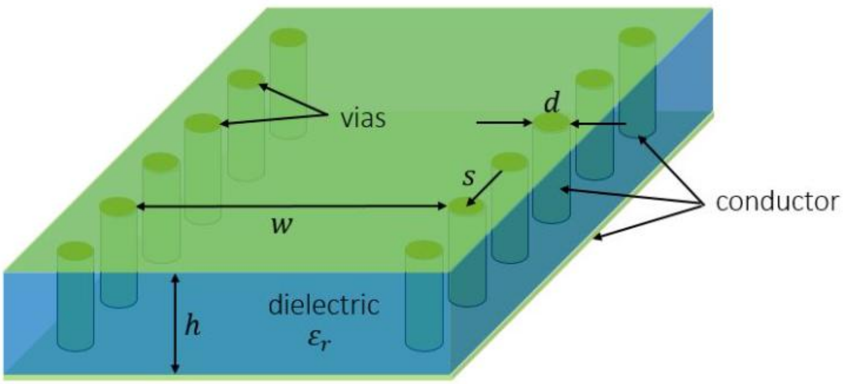

Figure II.3: Waveguide structure integrated into the substrate.

$$S \leq 2d \tag{II-1}$$

$$d < \frac{\lambda_g}{5} \tag{II-2}$$

Where: λ_g is the guided wavelength given by [II.13]:

$$\lambda_g = \frac{\pi}{\sqrt{\frac{(2\pi f)^2 \varepsilon_r}{c^2} - \left(\frac{\pi}{a}\right)^2}} \tag{II-3}$$

Another important parameter is the distance between the two rows of via, which defines the width of the SIW guide. This distance is represented by the parameter as in Figure II.4. This parameter is determined from the design equations of a waveguide rectangular. Where the cut-off frequency of a rectangular waveguide of the fundamental mode is the same as that of a waveguide integrated into the substrate, it is given by:

$$f_{c_{mn}} = \frac{c}{2\pi}\sqrt{\left(\frac{m}{a}\right)^2 + \left(\frac{n}{b}\right)^2} \tag{II-4}$$

Where:

c: The speed of light.

m, n: The number of modes.

a, b: The dimensions of the waveguide.

For a waveguide integrated into the substrate is considered as a waveguide conventionally filled with a RWG dielectric [II.14] the added dimension of the waveguide is calculated by the equation (II-6) and with the same cut-off frequency of the fundamental mode TE_{10}:

$$F_c = \frac{c}{2a} \tag{II-5}$$

$$a_d = \frac{a}{\sqrt{\varepsilon r}} \tag{II-6}$$

According to [II.15], the width of the waveguide SIW is given by:

$$a_s = a_d + \frac{d}{0.95s} \tag{II-7}$$

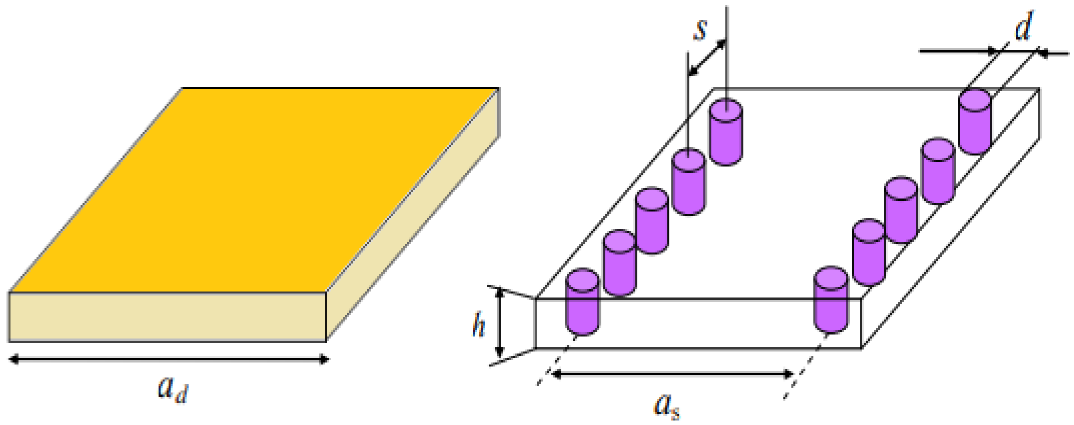

Figure II.4: Rectangular waveguide filled with a substrate with SIW configurations.

Figure II.5 shows the transverse field of view distributions of the waveguide dielectric and SIW at 5.5 GHz.

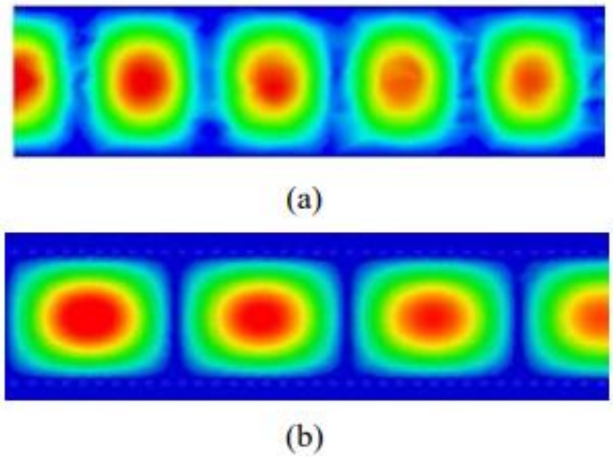

Figure II.5: The field distribution of the waveguide at 5.5 GHz. (a) waveguide rectangular, (b) SIW without transitions.

II.7. Transition from the microstrip lines to the waveguides integrated into the substrate

Since the SIW components and the planar circuits could be integrated on the same substrate, different effective transitions have been proposed to adapt waveguides with planar circuits [II.16]. We cite in particular the micro-conical ribbon transition (type) coplanar to the waveguide [II.17], easily achievable.

The microstrip line is one of the most used transmission lines in the design of microwave systems. A transition from the SIW to a micro-ribbon line has been proposed by Garlands in [II.18]. The topology of the structure is given in Figure II.6.

The transition can be broken down into two parts: the micro ribbon line and the waveguide rectangular.

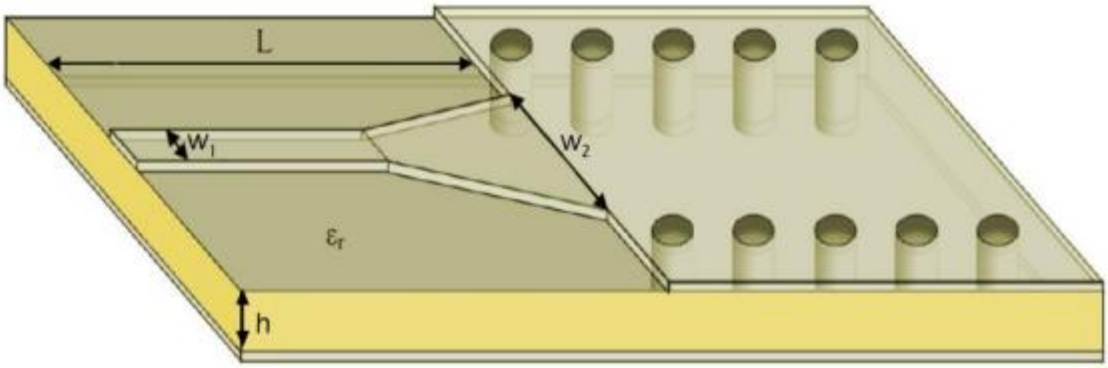

Figure II.6: Transition from a SIW to a microstrip line.

Figure II.7 shows the field lines in a rectangular waveguide and a line microstrip.

(a) (b)

Figure II.7: field lines (a) rectangular waveguide (b) a microstrip line [II.19].

II.8 Characteristic impedance

As shown in Figure II.8, this transition requires the calculation of the three parameters following:

1. The initial width of the micro-ribbon line $W1$,
2. the final width of the micro-ribbon line$W2$
3. the length L2 of the taper.

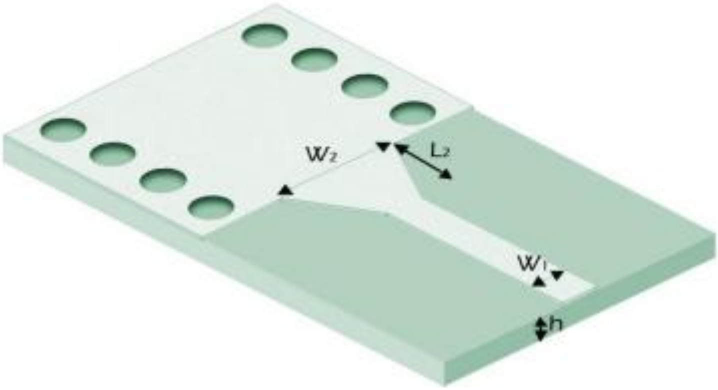

Figure II.8: geometric parameter of the transition.

$W1$ is generally chosen to obtain a characteristic impedance of 50 Ω. According to [II.20], the ratio $W1/h$ is calculated by the following equation

$$\frac{w_1}{h} = \begin{cases} \frac{8e^A}{e^{A-2}} \; for \; \frac{w_1}{h} < 2 \\ \frac{2}{\pi}\left[B - 1 - \ln(2B-1) + \frac{\varepsilon_r - 1}{2\varepsilon_r}\left\{\ln(B-1) + 0.39 - \frac{0.61}{\varepsilon_R}\right\}\right] \; for \; \frac{w_1}{h} > 2 \end{cases} \tag{II-8}$$

$$\mathrm{A} = \frac{Z_0}{60}\sqrt{\frac{\varepsilon_r + 1}{2}} + \frac{\varepsilon_r - 1}{\varepsilon_{r+1}}\left(0.23 + \frac{0.11}{\varepsilon_r}\right) \quad \text{and} \quad \mathrm{B} = \frac{377\pi}{2Z_0\sqrt{\varepsilon_r}} \tag{II-9}$$

with

Z_0 : Characteristic impedance of the micro ribbon line.

h : Thickness of the substrate.

ε_r : Relative permittivity of the substrate.

After calculating the ratio $W1/h$, we can deduce the value of $W1$ since we have the value of h.

According to [II.20], we calculate the value of $W2$ by equating the two equations (II.10) and (II.11).

$$\frac{1}{w_e} = \begin{cases} \frac{60}{\eta_h} \ln\left(8\frac{h}{w_2} + 0.25\frac{w_2}{h}\right) \\ \frac{120\pi}{\eta_h\left[\frac{W_2}{h} + 1.393 + 0.667\ln\left(\frac{w_2}{h} + 1.444\right)\right]} \end{cases} \tag{II.10}$$

$$\frac{1}{w_e} = \frac{4.38}{a_e} e^{-0.627\frac{\varepsilon_r}{\frac{\varepsilon_r+1}{2} + \frac{\varepsilon_r - 1}{2}\frac{1}{\sqrt{1+12\frac{h}{w_1}}}}} \tag{II.11}$$

With

we: The width of a waveguide that models the micro-ribbon line

ae: The width of a rectangular waveguide that provides the same cut-off frequency

η: The wave impedance

To determine the length $L2$ we calculate the median width between the micro ribbon line and the end of the post-transition [II.21, II.22]:

$$W_{\text{milieu}} = \frac{W1+W2}{2} \quad \text{(II-12)}$$

Then, we calculate the wavelength for this width and set the length to a quarter of the wavelength. So, we have to find the effective dielectric constant corresponds to this width of the micro-ribbon line by the equation (II-13):

$$\mathcal{E}e = \frac{\mathcal{E}r+1}{2} + \frac{\mathcal{E}r-1}{2}\frac{1}{\sqrt{1+12\frac{h}{W_{milieu}}}} \quad \text{(II-13)}$$

The cut-off wavelength is given by the following equation:

$$\lambda_c = \frac{1}{f_{c\sqrt{\mu_0 \varepsilon_0 \varepsilon_e}}} \quad \text{(II-14)}$$

After the calculation of the length $L2$, we must adapt our structure so that the line power supply is adapted to the SIW waveguide in order to obtain better transmission. For this, it is necessary to calculate the impedance of the SIW guide which is given by the equation next [II.23]:

$$Z_{pi} = Z_{TE}\,\frac{\pi^2 h}{8a_s} \quad \text{(II-15)}$$

λ_g is the guided wavelength. It is given by the following formula:

$$\lambda_g = \frac{\pi}{\sqrt{\frac{(2\pi f)^2 \varepsilon_r}{c^2} - \left(\frac{\pi}{a}\right)^2}} \quad \text{(II-16)}$$

Where Z_{TE} represents the impedance of the wave. For the TE_{10} mode, this gives:

$$Z_{TE} = j\frac{\omega}{\gamma} = \sqrt{\frac{\mu}{\varepsilon}} \times \frac{\lambda_g}{\lambda} \quad \text{(II-17)}$$

II.9. Implementation of SIW technology

SICs (Substrate Integrated Circuits) can be built using the structures synthesized integrated with other planar circuits such as the micro-ribbon line or others on the same dielectric substrate. Several passive and active SICs are mentioned in this section.

II.9.1. Passive circuits in SIW

Regarding passive circuits, most of the conventional microwave components have been implemented in SIW technologies. This solution generally makes it possible to obtain components with a reduced size compared to the waveguide functions classics. Some examples of passive components are shown in Figures II.9, such as the bandpass filter, the rectangular cavity, the coupler, and the SIW duplexer [II.24].

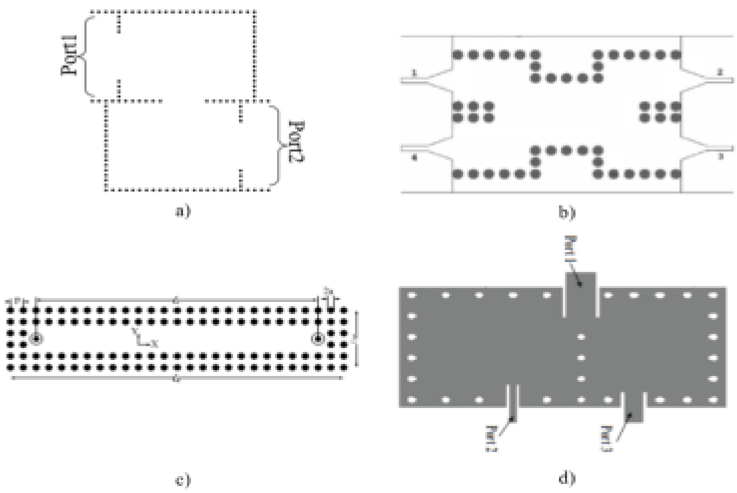

Figure II.9: Examples of SIW passive circuits, a) SIW bandpass filter, b) Coupler SIW, c) Rectangular guide SIW, d) Duplexer SIW.

II.9.2. Active circuits in SIW

The implementation of active components in SIW technology has attracted less attention compared to that of passive circuits. Nevertheless, new design possibilities towards a complete SoS (System-on-Substrate) integration are open. Essentially, the design and optimization of active circuits consist in integrating active devices in passive SIW circuits and connect them using the advantages of technology such as, for example, the low losses, the high insulation and a compact size to obtain good low-cost performance. Generally, one of the conductive faces of the SIW is used to postpone the active function, the connection being ensured by micro-ribbon lines. The recent developments of oscillators in 2012 [II.25], mixers [II.26] and amplifiers [II.27] are notable. Some examples are given in Figure II.10.

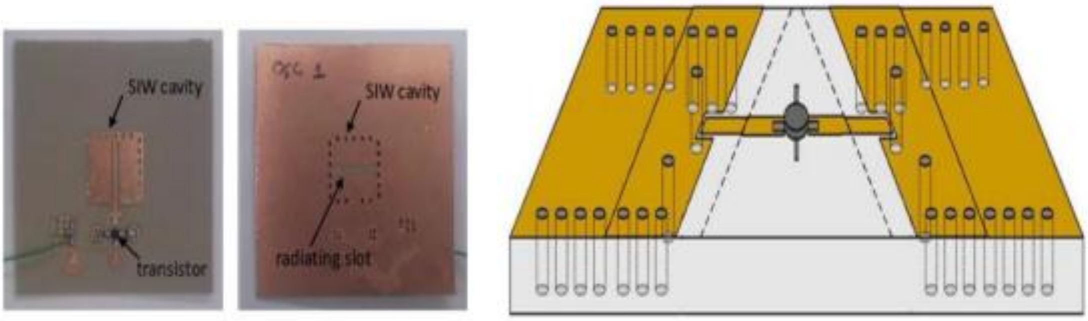

a) b)

Figure II.10: Examples of the active circuits SIW, a) SIW oscillator, b) SIW amplifier.

II.10. The HMSIW technique

Over the past decade, the HMSIW technology (Half Mode Substrate Integrated Waveguide) has been widely used to design more efficient filters. In 2006, the design of HMSIW was proposed by Wu and Hong [II.28]. The HMSIW is a guide of planar wave fabricated by implementing a wide extent of metal vias on a low-loss substrate with a metal coating, which is only half of the structure of a SIW and its dominant mode corresponds to about half of the mode10 mode, as illustrated in Figure II.11 It also offers the same propagation characteristics that SIW and keeps the advantages of a more compact size

It is known that when a SIW operates only in dominant mode, the field $\vec{E}$ has a maximum value in the vertical median plane along the direction of propagation, of so that the median plane can be considered as an equivalent magnetic wall. On the basis of this idea, we can divide the SIW into a fictitious magnetic wall and each half of the SIW becomes an HMSIW structure comprising metal vias with a network linear on one side, as shown in Figure II.12. On the opposite side, open circuit, the new structure can almost retain the original field distribution in its own part by because of its large width to height ratio [II.29].

The complexity of the manufacture is maintained at the same level as for the guide SIW wave. The HMSIW has been developed and widely used for the design of several components such as: antenna, coupler, duplexer and several filters have been designed on the base of the HMSIW.

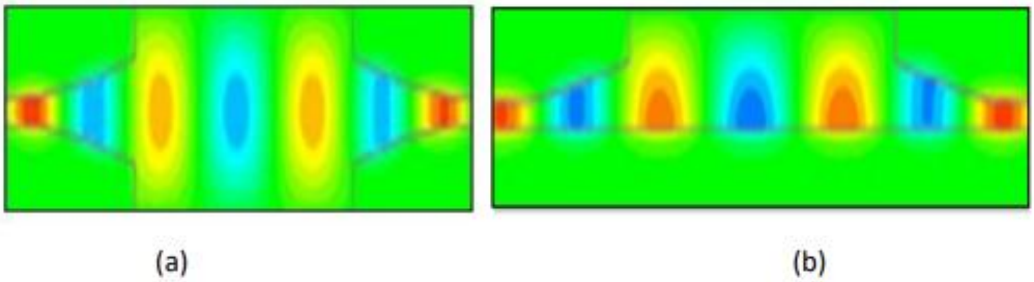

Figure II.11: Propagation of the electric field in a waveguide (a) SIW (b) HMSIW.

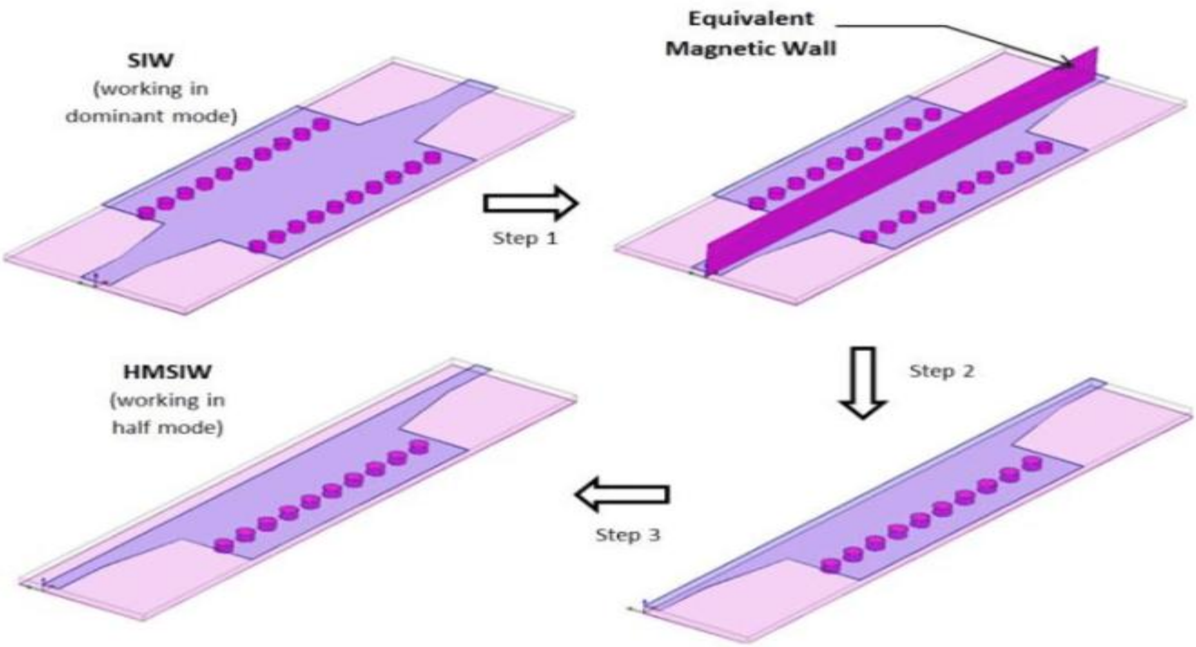

Figure II.12: Evolution of the HMSIW from the SIW.

The first electric mode fields of the SIW and the HMSIW are illustrated in Figure II.13.

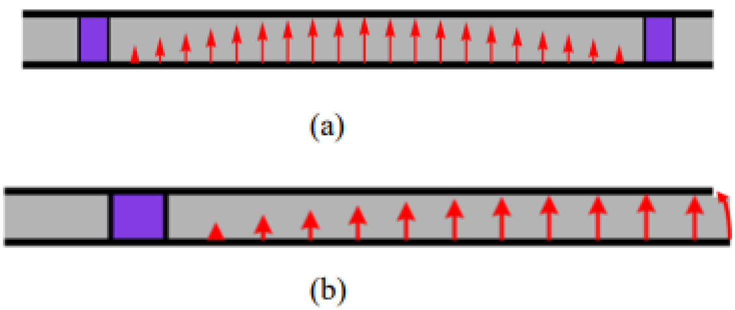

Figure II.13: Electric field of SIW and HMSIW (a) SIW mode TE_{10} mode, (b) mode HMSIW TE_{10}.

II.11. Bandpass filter integrating HMSIW and low-pass filter

Figure II.14 shows the synthesis diagram of the proposed bandpass filter, made up of a low-pass filter and a high-pass filter. The passband frequencies of the low-pass filter and the high-pass filter are the frequencies of the upper and lower end bands of the bandpass filter, respectively. Meanwhile, the group delay of the designed filter is the sum of those of the low-pass filter and the high-pass filter.

The filter is simulated and designed with CST microwave studio software, and manufactured on FR-4 substrate.

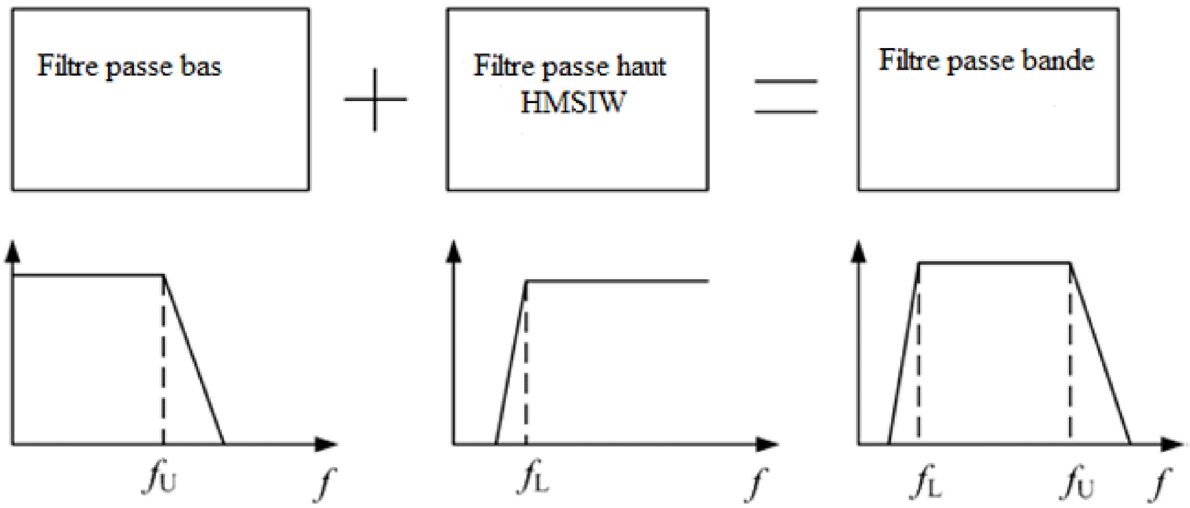

Figure II.14: Diagram of the bandpass filter formation process [II.30].

Figure II.15 illustrates the HMSIW configuration with a cutoff frequency of fL GHz, where D and S are the diameter and period of the metal feedthroughs, and Wrepresents the width of HMSIW which determines its cutoff frequency. This cutoff frequency is also that of the bandpass filter's underside. The SIW-microstrip transition is used to connect a 50 Ω test system, where W_{50} and W_{taperis} are the widths at the two ends of the microstrip cone and L_{taperis} the length of the cone.

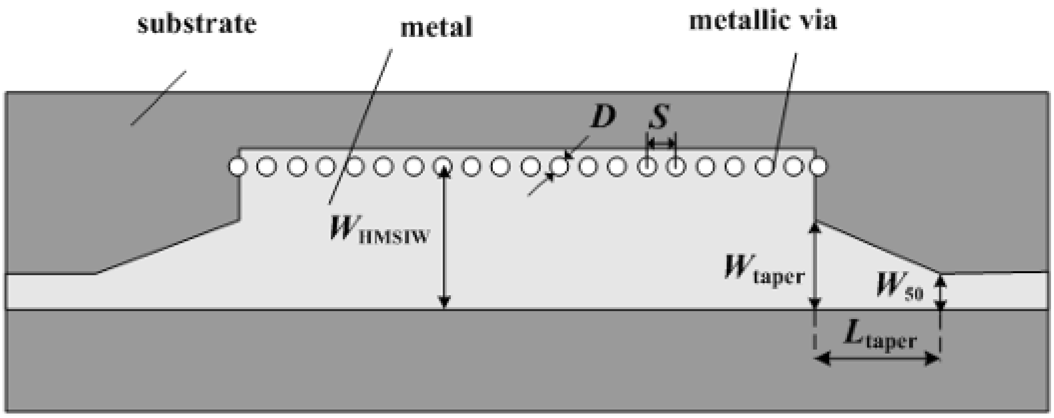

Figure II.15: HMSIW configuration and dimensions [II.30].

II.12. HMSIW microwave filters

Half-mode substrate integrated waveguides (HMSIW) can be designed on planar substrates. These structures have been used to implement planar resonators and filters with low insertion losses, a high quality factor and a low price that makes the volume size compact compared with that of bulky waveguide filters. The HMSIW concept is essential for filter design, and it is very practical to engrave tunable elements on the surface of the HMSIW waveguide [II.30-II.31].

The filter bandwidth is limited by the HMSIW cut-off frequencies because the electromagnetic wave cannot be transmitted when the frequency is below the cut-off frequency. Usually, the cut-off frequency is reduced by increasing the width of the HMSIW, but this will also increase the filter size. The filters studied in references [II.32-II.35] have a low cut-off frequency. Figure II.16 shows some examples of microwave components in HMSIW.

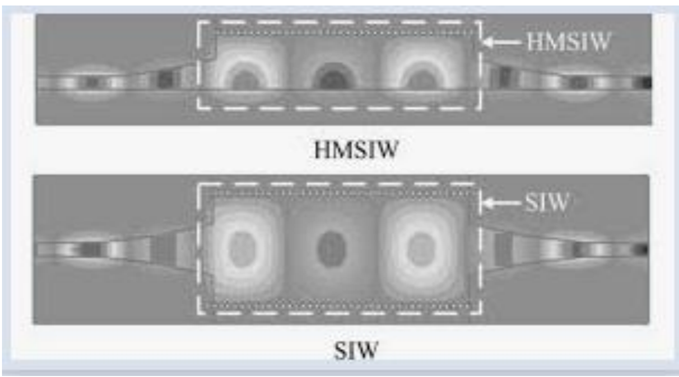

(a) SIW and HMSIW couplers.

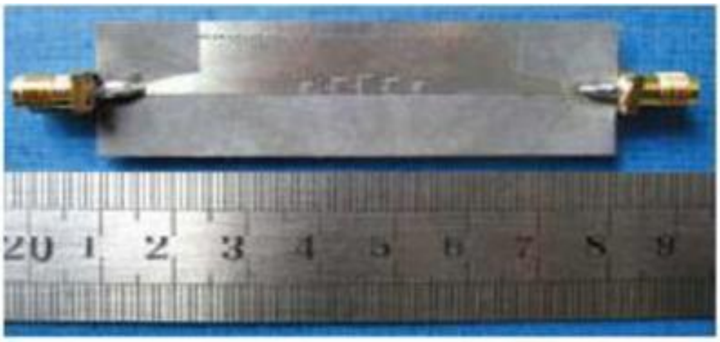

(b) HMSIW filter.

Figure II.16: Some examples of microwave components made using HMSIW technology.

II.13. Field theory in a HMSIW guide

Due to the growing demand for wireless communications in recent decades, efforts have been made to reduce the size and cost of microwave circuits. Typically, the size of a SIW circuit is much larger than that of a microstrip line or a coplanar CPW line. This could be advantageous for millimeter-wave applications, since the manufacturing tolerance of PCB processes will be much more relaxed compared to the size and processing of circuit parameters. However, the large size of SIW components also poses a problem for their applications at low frequencies. In order to reduce the size of SIW circuits, new techniques have been proposed and demonstrated such as HMSIW [II.36, II.37] Recently, the half-mode SIW structure, has shown that the SIW concept can be cut in half by a fictitious magnetic wall and each SIW half becomes an HMSIW structure. The new structure can practically retain the original field distribution [II.38, II.39].

The components of the $TEmn$ mode field in a SIW (assuming that the width of a conventional SIW guide is $2w$), can be calculated, exploiting the theory of conventional waveguide fields [II.40, II.41]:

$$E_x = A_{mn}\frac{K_y}{\varepsilon}\cos[K_x(W-x)]\sin\left[K_y\left(y-\frac{h}{2}\right)\right]e^{-jk_zZ} \quad \text{(II-18)}$$

$$E_y = A_{mn}\frac{K_x}{\varepsilon}\sin[K_x(W-x)]\cos\left[K_y\left(y-\frac{h}{2}\right)\right]e^{-jk_zZ} \quad \text{(II-19)}$$

$$E_Z = 0$$

$$H_x = A_{mn}\frac{K_xK_z}{\omega\mu\varepsilon}\sin[K_x(W-x)]\cos\left[K_y\left(y-\frac{h}{2}\right)\right]e^{-jk_zZ} \quad \text{(II-20)}$$

$$H_y = A_{mn}\frac{K_yK_z}{\omega\mu\varepsilon}cos[K_x(W-x)]\,sin\left[K_y\left(y-\frac{h}{2}\right)\right]e^{-jk_zZ} \quad \text{(II-21)}$$

$$H_Z = A_{mn} \frac{K_x K_z}{\omega\mu\varepsilon} \cos[K_x(W - x)] \cos\left[K_y\left(y - \frac{h}{2}\right)\right] e^{-jk_z Z} \quad \text{(II-22)}$$

with:

$$K_x = \frac{m\pi}{2\omega} \quad \text{(II-23)}$$

$$H_y = \frac{n\pi}{h} \quad \text{(II-24)}$$

$$K_Z^2 = K^2 - [\,(\frac{m\pi}{2\omega})^2 + (\frac{n\pi}{h})^2\,] \quad \text{(II-25)}$$

Or

$$-w \le x \le w, -\frac{h}{2} \le y \le \frac{h}{2} \quad \text{(II-26)}$$

The term $y - \frac{h}{2}$ is close to 0 since the substrate is very thin. This gives :

$$sin\left[K_y\left(y - \frac{h}{2}\right)\right] \approx 0 \text{ et } cos\left[K_y\left(y - \frac{h}{2}\right)\right] \approx 1 \quad \text{(II-29)}$$

Based on the previous equations, the field components of the dominant half-mode inside the HMSIW can be given by the following expressions [II.42]:

$$E_{y(0.5,0)} = \mathrm{A}k_x \sin k_x(w - x)\, e^{-jk_z Z} \quad \text{(II-30)}$$

$$H_{x(0.5,0)} = \mathrm{A}k_x \sin k_x(w - x)\, e^{-jk_z Z} \quad \text{(II-30)}$$

with:

$$\mathrm{K} = \frac{\pi}{2(w-a)} \quad \text{(II-31)}$$

$$k_y = 0$$

$$K_Z = \sqrt{K_0^2 \varepsilon_r - \frac{\pi^2}{4(w-a)^2}} \quad \text{(II-32)}$$

Or:

- $0 \le x \le w,$
- The index (0.5, 0) represents the half-mode,
- ω is the pulsation,
- a is the position of the maximum electric field along the cross-section of the HMSIW along the x coordinate.

In addition, the cutoff frequency and phase constant in the dominant mode of a HMSIW can be calculated by [II.40]:

$$f_{c,TE_{0.5,0}} = \frac{c}{4\sqrt{\varepsilon_r}\,W_{eff,HMSIW}} \tag{II-33}$$

In which, the effective width of $HMSIW$, $W_{eff,HMSIW}$est given by:

$$W_{eff,HMSIW} = \frac{W_{SIW}}{2} + \Delta W \tag{II-34}$$

$$W'_{eff,HMSIW} = \mathrm{W} - 0.54\frac{d^2}{s} + 0.05\frac{d^2}{2W} \tag{II-35}$$

The additional width $\Delta W$of a HMSIW can be estimated by [II.40]:

$$\frac{\Delta W}{h} = \left(0.05 + \frac{0.3}{\varepsilon_r}\right).\ln\left(0.79 + \frac{W\prime_{eff,HMSIW}}{h^3} + \frac{104W\prime_{eff,HMSIW}-261}{h^2} + \frac{38}{h} + 2.77\right) \tag{II-36}$$

II.14. Comparison of miniaturized SIW transmission lines

A study presents comparing several miniaturization techniques, including, in which they compares the sizes of these guides and their compression ratios in the following table.

Table II.1: Lateral dimensions and compression ratio of each miniaturized SIW.

	SIW	HMSIW	RSIW	CFSIW	TFSIW
Lateral dimension [mm]	5	3	3.5	2.9	2.9
compression ratio	1	0.6	0.7	0.58	0.58

The wide lateral dimensions and compression ratio of each line are listed in Table II.1. FSIWs achieve the highest compression ratio.

II.15. Conclusion

In this chapter, we explored the principles and advantages of Substrate Integrated Waveguide (SIW) and its derivative, the Half-Mode SIW (HMSIW), which are pivotal in the design of modern compact and efficient microwave components. SIW technology offers the benefits of traditional waveguides—such as low loss and high-quality factor—while being compatible with planar fabrication processes, enabling easier integration with other circuit elements. The design parameters, including via dimensions and spacing, play a crucial role in minimizing losses and ensuring proper wave confinement.

HMSIW, as an evolution of SIW, allows for further miniaturization while preserving desirable propagation characteristics, thanks to the magnetic wall principle. It supports the development of compact, cost-effective, and high-performance components like filters, couplers, and antennas. The chapter also highlighted various transition techniques between microstrip lines and SIW/HMSIW to ensure efficient signal transmission across integrated systems.

By understanding these technologies, designers are better equipped to develop advanced microwave systems that meet the stringent requirements of modern telecommunications.

References

[II.1] **F.Benzarga** ‘’ étude et conception des réseaux d’antennes a ouverture progressive pour l’imagerie passive et la technologie SIW Modélisation par la méthode des éléments finis 2D,’’Ph.D dissertation. Faculté de technologie, université de Tlemcen, 2016.

[II.2] **Z. Li, K. Wu**.(2008,Feb).24-GHz Frequency-Modulation Continuous-Wave Radar FrontEnd System-on Substrate. IEEE Trans. Microw. Theory Tech., vol. 56, no. 2.

[II.3] **N. A.Smith.** ‘’Substrate Integrated Waveguide Circuits and Systems,’’Ph.d dissertation, Dept of Electrical & Computer Engineering McGill, University Montréal, Québec, Canada,2010.

[II.4] **M. A. Rabah, M. Abri, H.A Badaoui, J. Tao, and T.H.** (2016). Vuong Compact Miniaturized Half-Mode Waveguide/High Pass-Filter Design Based on SIW Technology Screens Transmit-IEEE C-Band signals. Microwave Opt Technol Lett. 58:414–418.

[II.5] **K.Dong, J.Mo, Y.He, Z.Ma, X.Yang**. (2016, October).design of a millimeter-wave wideband band pass filter with novel-slotted substrate integrated waveguide. Microwave and optical technology letters.Vol. 58, No. 10.

[II.6] **M.reza, F.Ehsan, Z.Jahromi, R.Basiri.** (2018, August). A compact semi-open wideband SIW horn antenna for K/Ku band applications. AEU - International Journal of Electronics and Communications.Vol.92, pp. 15-20.

[II.7] **T.Agrawal, Shweta, Srivastava, Ku.** (2018,April). band pattern reconfigurable substrate integrated waveguide leaky wave horn antenna. AEU - International Journal of Electronics and Communications, 87, pp. 70-75.

[II.8] **D. Deslandes and K.Wu.** (2006, Jun). accurate Modeling wave Mechansms, and design consdiration of substrat waveguide. IEEE Transaction on microwave theory and techniques.vol54, no 6.

[II.9] **M. Ando, J. Hirokawa and Al.** (1997). Novel single-layer waveguides for high-efficiency millimeter-wave arrays. IEEE millimeter waves conference proceedings, pp.177180.

[II.10] **Y. Cassivi, L. Perregrini, P. Arcioni, M. Bressan, K. Wu, and G. Conciauro.** (2002). Dispersion characteristics of substrate integrated rectangular waveguide. IEEE Microwave and Wireless Components Letters. No. 12, pp.333-335.

[II.11] **Y. Cassivi, L. Perregrini, P. Arcioni, M. Bressan, K. Wu, and G. Conciauro.** (2002, September). Dispersion characteristics of substrate integrated rectangular waveguide IEEE Microwave Wireless Compon. Lett. vol. 12, pp. 333–335.

[II.12] **D. Deslandes and W. Ke, Accurate.** (2006). modelling, wave mechanisms, and design considerations of a substrate integrated waveguide. IEEE Transactions on Microwave Theory and Techniques. vol. 54, pp. 2516-2526.

[II.13] **J. E. Rayas-Sanchez and V. Gutierrez-Ayala.** (2008,Jun). A general EM-Based design procedure for single-layer substrate integrated waveguide interconnects with microstrip Transitions. IEEE MTT-S Int. Microwave Symp. Dig., Atlanta, GA, pp. 983-986.

[II.14] **J. E. Rayas-Sanchez and V. Gutierrez-Ayala.** (2008,Jun). A general EM-Based design procedure for single-layer substrate integrated waveguide interconnects with microstrip Transitions. IEEE MTT-S Int. Microwave Symp. Dig., Atlanta, GA, pp. 983-986.

[II.15] **E.PucciGap** ‘’Waveguide Technology for Millimeter Wave Applications and Integration with Antennas,’’Ph.D dissertation. Dept of Signals and Systems Chalmers, University of Technology G¨oteborg, Sweden,2013.

[II.16] **H. Baudrand,** ‘’Méthode snumériquesen propagation,’’ Conference proceedings, 20th EuropeanMicrowave Conference, vol. 20, Sept.1985.

[II.17] **D.Deslandes and K.Wu.** (2005, Aug). Analysis and design of current probe transition from groundedcoplanar to substart rectangular waveguide. IEEE Transaction on microwave theory and techniques.vol 53, no 8.pp2487-2494.

[II.18] **Y. Cassivi, L. Perregrini, P. Arcioni, M. Bressan, K. Wu, and G. Conciauro** (2002, September) Dispersion characteristics of substrate integrated rectangular waveguide. IEEE Microwave Wireless Compon Lett. vol. 12, pp. 333–335.

[II.19] **F.Benzarga** ‘’ étude et conception des réseaux d’antennes a ouverture progressive pour l’imagerie passive et la technologie SIW Modélisation par la méthode des éléments finis 2D,’’Ph.D dissertation. Faculté de technologie, université de Tlemcen, 2016.

[II.20] **D. Deslandes.** (Feb.2001).Design equations for tapered microstrip-to-substrate integratedwaveguide. transitions IEEE MTT-S International Microwave Symposium Digest (MTT), California.

[II.21] **D. Deslandes and K.Wu.** (Feb, 2001) Integrated micro strip and rectangular wave guide in planar form.IEEE Microw Wirless compon.lett. vol.11, no 2, pp 68-70.

[II.22] **F.Xu, K .WU.** (2005, Jan).Guide-wave and leakage characteristics of substart integrate waveguide. IEEE Trans Microw Theory Tech. vol 53, no.1, pp.66-73.

[II.23] **M. Georgiadis, A. Wu, K., Bozzi.** (June, 2011).Review of substrate-integrated waveguide circuits and antennas.Microwaves Antennas & Propagation IET. vol. 5, no. 8, pp. 909-920.

[II.24] **D. Makris, K. Voudouris, N. Athanasopoulos,** ''Design and Development of 60 GHz Millimeter-wave Passive Components using Substrate Integrated Waveguide Technology,'' 2nd Pan-Hellenic Conference on Electronics and Telecommunications PACET 12, March .2012.

[II.25] **Y. Liu, X.Hong, T.Tao, W.Ling, Wang and F.Xiao.** (2012,May) A SIW-based Concurrent dual-band oscillator.Microwave and Millimeter Wave Technology (ICMMT).vol. 1, pp. 1-4.

[II.26] **J. Wu, K. Xu.** (2005, June). A sub harmonic self-oscillating mixer using substrate integrated waveguide cavity for millimeter-wave application. IEEE MTT-S Int. Microwave Sympppp. 1-4.

[II.27] **M. Shahabadi, M.Abdolhamidi.** (2008, Dec). X-Band Substrate Integrated Waveguide Amplifier. Microwave and Wireless Components Letters, IEEE. vol. 18, no. 12, pp. 815-817.

[II.28] **W. hong, B et al.,** ''Half mode substrate integrated waveguide: A new guided wave structure for microwave and millimeter wave application,'' in Proc. Joint 31stInt.Infrared Millimeter Wave Conf./14th Int. Terahertz Electron. Conf.,Shanghai, China, pp. 18–22, Sep. 2006.

[II.29] **B. Liu, W.Hong, Y.Qing Wang, Q-H. Lai, and K.Wu.** (2007,January).Half Mode Substrate Integrated Waveguide (HMSIW) 3-dB Coupler. IEEE Microwave And Wireless Components Letters.Vol. 17, N°. 1.

[II.30] **He. Fanfan,** ''Innovative microwave and millimetre-wave components and sub-sysytems based on substrate integration technology,'' Ph.D dissertation, université de montréal,2011

[II.31] **D.Yan,** ''Miniaturization Techniques of Substrate Integrated Waveguide Based on Multilayered Printed Circuit Board Platform,'' Ph.D dissertation, université de montréal, 2011.

[II.32] **Y. D. Dong, T.Yang, T.Itoh.** (2009).Substrate Integrated Waveguide Loaded by Complementary Split-Ring Resonators and Its Applications to Miniaturized Waveguide Filters.IEEE Transactions on Microwave Theory and Techniques. pp: 2211-2223.

[II.33] **S. Nathan,** ‘’Substrate integrated Waveguide Circuits and Systems,’’, Ph.D dissertation, université Montréal, Québec, Canada, 2010.

[II.34] **N. Grigoropoulos, B. S. Izquierdo, and P. R. Young.** (2005).Substrate integrated folded waveguides (SIFW) and filters. IEEE Microw Wireless Compon Lett. vol. 15, no. 12, 829 831.

[II.35] **G. Jonathan,** ‘’Etude de filtres hyperfréquences SIW et hybride planaire SIW en technologie LTCC,’’ Ph.D dissertation, université de bretagne occidentale, 2012.

[II.36] **W. Che, L. Geng, K. Deng, and Y. L. Chow.** (2008).Analysis and experiments of compact folded substrate-integrated waveguide. IEEE Trans. Microw. Theory Tech.,vol. 56, no. 1, 88 93.

[II.37] **S.Cohn,** (1999).“Parallel-coupled transmission-line resonator filters” IRE Trans. Microwave Theory Tech., vol. 10, no. 4, pp. 223–231.

[II.38] **Q.Lai, C.Fumeaux, W.Hong, and R.Vahldieck.** (2009,August).Characterization of the Propagation Properties of the Half-Mode Substrate Integrated Waveguide. IEEE Transactions On Microwave Theory And Techniques, VOL. 57, NO. 8.

[II.39] **G. Matthaei, L. Young and E. M. T. Jones** “ Microwave filters, impedance-matching networks, and coupling structures’’ Boston, Artech House, 1980.

[II.40] **Yuanqing .Wang, Wei. Hong.** (2007,April).Half Mode Substrate Integrated Waveguide (HMSIW) Bandpass Filter. IEEE microwave and wireless components letters, vol. 17, NO. 4.

[II.41] **B.Liu, W.Hong, Z.Hao, et K.Wu,** ‘’Substrate integrated waveguide 180-degree narrow-wall directional coupler’’. Asia-Pacific Microwave Conference Proceedings, 1. (2005).

[II.42] **W.Hong, B.Liu, Y.Wang, H.Q.Lai, et K.Wu,** ‘’Half mode substrate integrated waveguide: A new guided wave structure for microwave and millimeter wave application,’’. Joint 31st International Conference on Infrared and Millimeter Waves and14th International Conference on Terahertz Electronics. 219, (2006).

CHAPTER III

SIW/HMSIW bandpass filters loaded with CHMCs

III.1. Introduction

Chapter III explores the design and simulation of bandpass filters, essential components in modern communication systems. Traditionally, microstrip technology has been a primary method for designing these filters due to its planar configuration, ease of fabrication, and compatibility with other microwave components. Despite these advantages, microstrip filters suffer from limitations such as higher insertion loss and reduced power handling capabilities, which can compromise their effectiveness in high-frequency applications.

To overcome these challenges, this work employs Substrate Integrated Waveguide (SIW) technology, which offers a compelling alternative. SIW merges the benefits of microstrip and conventional waveguide technologies, delivering lower loss, a higher quality factor, and improved power handling while preserving a planar structure. This makes SIW an ideal choice for high-performance bandpass filter designs. Furthermore, Half-Mode SIW (HMSIW) is introduced as a variant that halves the size of the SIW structure without significant performance degradation, enhancing miniaturization efforts for compact filter applications.

The core innovation of this chapter is the development of a novel metamaterial structure, the Complementary Hexagonal Metamaterial Cell (CHMC), based on hexagonal complementary split ring resonators (CSRR). Metamaterials, with their unique ability to manipulate electromagnetic waves, are particularly valuable in filter design. A key benefit of using the CHMC cells is to miniaturize and reduce the size of the filter, enabling significant compactness while enhancing performance. This addresses the critical need for space-efficient designs in modern electronic devices.

This chapter is organized as follows:

It begins with a brief introduction to the concept of metamaterials, followed by the presentation of the CHMC cell. Subsequently, two SIW-based bandpass filters, incorporating different numbers of CHMC cells, are designed and analyzed to evaluate the influence of cell configuration on filter performance. Next, HMSIW-based filters utilizing these cells are introduced and examined, highlighting the advantages of a more compact design. Finally, a dual-band filter employing CHMC cells of varying sizes is presented, demonstrating the flexibility and potential of this metamaterial approach in achieving multiple passbands.

III.2. Complementary hexagonal metamaterial cells

Metamaterials are artificially engineered structures designed to exhibit electromagnetic properties not typically found in natural materials. A common building block for microwave metamaterials is the Split-Ring Resonator (SRR), known for its resonant magnetic response. Its counterpart, the Complementary Split-Ring Resonator (CSRR) exhibits a resonant electric response and is often implemented by etching slots in conductive surfaces, such as the ground plane of microstrip circuits, forming a Defected Ground Structure (DGS).

Leveraging these concepts, this dissertation proposes several novel Bandpass Filters (BPFs). While each BPF design possesses unique characteristics, they share a common foundation: the utilization of a newly proposed Complementary Hexagonal Metamaterial Cell (CHMC) functioning as a DGS. The CHMC design is derived from a conventional hexagonal-CSRR, similar to that presented in [III.1] (Figure III.1 (a)). However, a key modification distinguishes the proposed CHMC: the inner ring of the traditional hexagonal-CSRR is removed, and its resonant behavior is instead influenced by introducing two inward-directed arms positioned on either side of the outer ring's gap (Figure III.1 (b)).

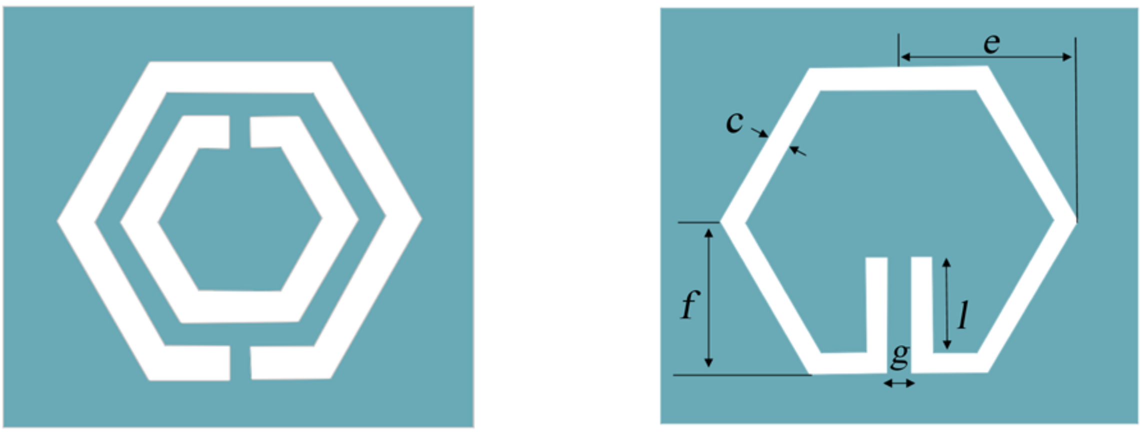

(a) (b)

Figure III.1: The layout of: (a) A hexagonal-CSRR. (b) A CHMC unit.

This innovative CHMC geometry offers significant advantages. Firstly, it effectively increases the electrical length, contributing to the miniaturization of the overall BPF structures. Secondly, the design is simplified to a single modified ring, potentially easing fabrication and modeling. Finally, the length of the introduced arms provides a straightforward mechanism for controlling the cell's resonant frequency, thereby enabling precise tuning of the filter's target passband.

III.2.1. Validating Metamaterial Behavior via Effective Parameter Extraction

A crucial objective of this study is to demonstrate that the proposed filter structures function as effective metamaterials within their operational frequency bands. A defining characteristic of many resonant metamaterials is the exhibition of a negative effective refractive index (n) near their resonance frequency. This counter-intuitive property typically arises when both the effective permittivity (ε_{eff}) and the effective permeability (μ_{eff}) of the structured medium simultaneously become negative over a common frequency range. Therefore, computationally or experimentally determining these effective parameters, particularly verifying the negative refractive index condition, serves as a standard method to confirm the metamaterial nature of a designed device.

Several techniques exist for extracting the effective permittivity and permeability from simulated or measured scattering parameters (S-parameters), primarily the reflection (S11) and transmission (S21) coefficients. Each extraction method possesses distinct advantages and limitations. The choice of method depends on factors such as the nature of the S-parameter data (simulated vs. measured), the physical dimensions of the sample or unit cell, the specific dielectric properties being sought, computational efficiency, and the desired accuracy of the retrieved parameters.

III.2.1.1. Extraction by the Nicolson-Ross-Weir method

The Nicolson-Ross-Weir (NRW) extraction method is based on inverting Fresnel formulae that describe the normal reflection and transmission coefficients of a composite medium layer using its wave impedance and refractive index, which can be used to calculate the average permittivity and permeability. The NRW technique, also known as the distributed impedance method, is used to characterize natural materials as well as composite (granular) materials with a highly dense grain arrangement numerically and experimentally [III.2, III.3]. Smith et al. were the first to use this approach in the context of metamaterials [III.4]. The disadvantage of this method is the fact that only one propagating mode must exist at the frequency considered. In addition, the extraction of the effective parameters will be possible in the case where the incident wavelength is greater than the sizes and distances between the elementary constituents of the composite medium.

The NRW method is based on a simple interference calculation that determines the transmission and reflection of a layer of material as a function of its effective index, effective impedance, and thickness. Smith proved that by inverting the Fresnel equations we can obtain the values of n_{eff} and z_{eff} as a function of the simulated layer thickness d at the coefficients of transmission $t' = s_{21}$ and reflection $r = s_{11}$ [III.4]:

$$Re(n_{eff}) = \pm Re(\frac{\arccos\left(\frac{1}{2t'}\left[1-\left(r^2-t'^2\right)\right]\right)}{kd}) + \frac{2\pi m}{kd} \quad \text{(III-1)}$$

$$Im(n_{eff}) = \pm Im(\frac{arccos\left(\frac{1}{2t'}\left[1-\left(r^2-t'^2\right)\right]\right)}{kd}) \quad \text{(III-2)}$$

$$z_{eff} = \pm\sqrt{\frac{(1+r)^2-t'^2}{(1-r)^2-t'^2}} \quad \text{(III-3)}$$

To check the effect of the metamaterial on the device, it is necessary to extract and establish the effective refractive index (n_{eff}). This extraction is done by following a few steps.

1) Export the simulation results of coefficients s21 and s11 from CST or HFSS.
2) Import these parameters into MATLAB as columns.
3) Using MATLAB functions to enter NRW equations and apply them to the imported [S] parameters.
4) Examining the real and imaginary parts of the effective refractive index that will result from this program.

III.3. SIW bandpass filters loaded with CHMCs

Building upon the defined Complementary Hexagonal Metamaterial Cell (CHMC), this section details the first set of proposed Bandpass Filters (BPFs). These initial designs employ Substrate Integrated Waveguide (SIW) as the core guiding structure, which is then modified by loading it with varying numbers of CHMCs to achieve the desired filtering response.

The first specific example, presented in Figure III.2, integrates two identical CHMCs within the SIW framework. These CHMCs are realized as etched patterns on the top metallic surface of the substrate. Their orientation is deliberately configured with the gap openings pointing towards the structure's center. It is important to note that the substrate material, RT/Duroid

5880 with a relative permittivity of 2.2, a loss tangent of 0.009, and a thickness (h) of 0.508 mm, remains constant for this and all subsequent filter designs presented herein. This first SIW-CHMC filter achieves effective miniaturization, occupying a physical area of only 8 mm × 14.48 mm. For precise replication and analysis, the detailed dimensions of the SIW cavity and the CHMC elements are provided in Table III.1.

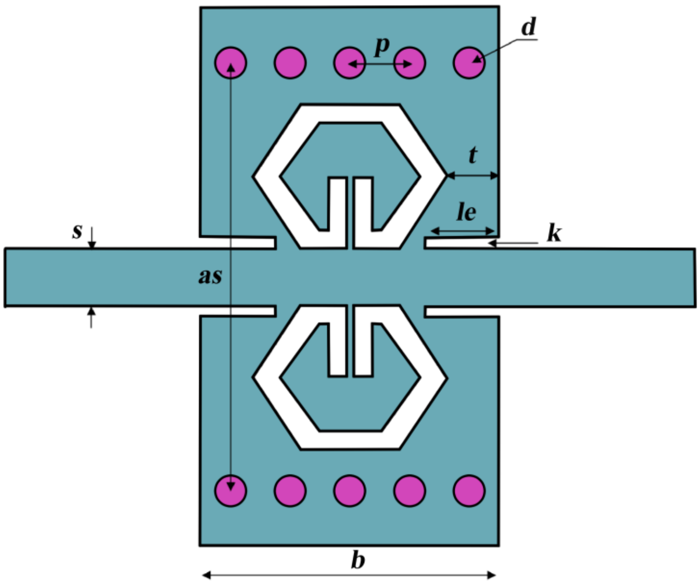

Figure: III.2: Top view of the SIW BPF loaded with two CHMCs.

Table III.1: The dimensions of the SIW bandpass filter loaded with two CHMCs (unit: mm).

Parameters	Dimensions	Parameters	Dimensions
as	11.52	k	0.3
d	0.8	e	2.63
p	1.6	f	1.95
b	8	c	0.5
s	1.53	g	0.2
h	0.508	l	1.9
le	2	t	1.37

The simulated frequency response of the dual-CHMC SIW filter is illustrated in Figure III-3, showing the reflection (S_{11}) and transmission (S_{21}) coefficients over the 2 GHz to 9 GHz range. Primary simulations were performed using CST Microwave Studio. Crucially, these results were corroborated through independent simulations employing HFSS software, yielding excellent agreement despite the inherent differences in the simulators' numerical techniques, thus bolstering confidence in the predicted behavior. The S-parameter analysis confirms the intended narrow bandpass filter operation. Resonance occurs at 5.8 GHz, where the filter demonstrates favorable characteristics: a deep return loss (S11 ≈ -36 dB) indicating good impedance matching, and minimal insertion loss (S21 ≈ 0.05 dB) signifying efficient signal transmission within the passband. The filter also provides substantial out-of-band rejection, with stopbands (S21 < -10 dB) spanning 2 GHz–4.9 GHz and 6.5 GHz–9 GHz. Maximum rejection levels within these bands are approximately -27 dB (at 2 GHz) and -47 dB (at 8 GHz).

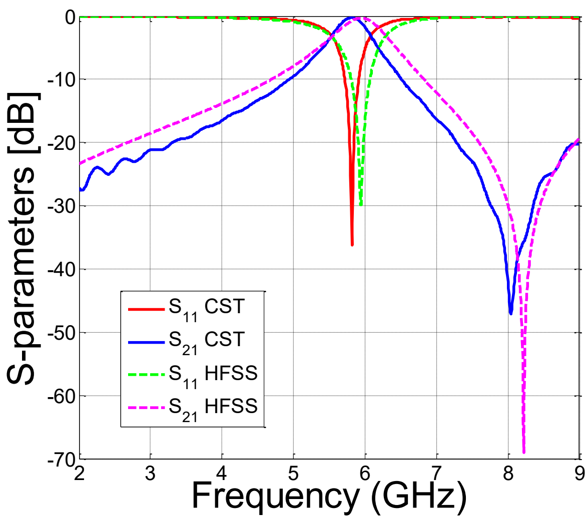

Figure III.3: Simulation results of the reflection and transmission coefficients for SIW BPF loaded with two CHMCs.

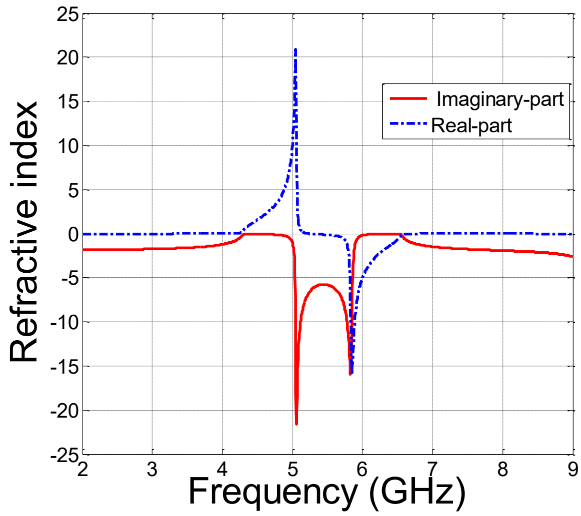

Figure III.4: The real and imaginary parts of the effective refractive index of the SIW BPF loaded with two CHMCs.

The metamaterial characteristics of the dual-CHMC filter are confirmed by analyzing its effective refractive index (n), extracted via the Nicolson-Ross-Weir (NRW) method. As shown in Figure III.4, both the real and imaginary parts of ' n ' simultaneously attain negative values near the 5.8 GHz resonance. This negative refractive index signature is a definitive indicator of metamaterial operation.

The subsequent Bandpass Filter (BPF) design presented builds upon the previous configuration, employing similar design principles but incorporating four Complementary Hexagonal Metamaterial Cells (CHMCs) instead of two. These four CHMCs are arranged symmetrically in two pairs along the Substrate Integrated Waveguide (SIW) structure, as illustrated in Figure III.5. A critical design parameter in this topology is separation distance, denoted as 'X', between the two CHMC pairs. This spacing significantly influences the electromagnetic coupling between the resonator pairs. Through parametric simulation studies varying 'X', an optimal value of X = 5.1 mm was determined for the desired filter response. While the inclusion of additional CHMCs is intended to enhance filter, it inherently increases the overall physical dimensions. Consequently, the effective footprint of this four-CHMC filter expands to 18.36 mm × 14.8 mm.

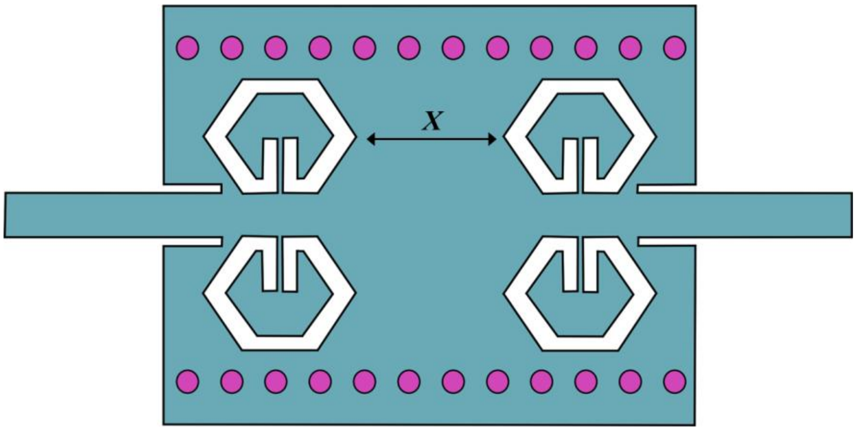

Figure III.5: Top view of the SIW BPF loaded with four CHMCs, where X=5.1 mm.

Figure III.6 displays the simulated S-parameters (S_{11} and S_{21}) for the SIW BPF incorporating four CHMCs. These results were generated using CST Microwave Studio and subsequently validated via simulations in HFSS, confirming consistency. A comparative analysis with the previous two-CHMC filter reveals a primary consequence of using four resonators: a noticeably wider operational bandwidth. Specifically, the reflection coefficient (S11) remains below -10 dB over the frequency range from 6.0 GHz to 6.35 GHz, indicating good matching within this passband. However, the increased number of resonators and associated coupling effects induce a shift in the center frequency to approximately 6.2 GHz. At this frequency, the minimum S11 achieved is -28 dB.

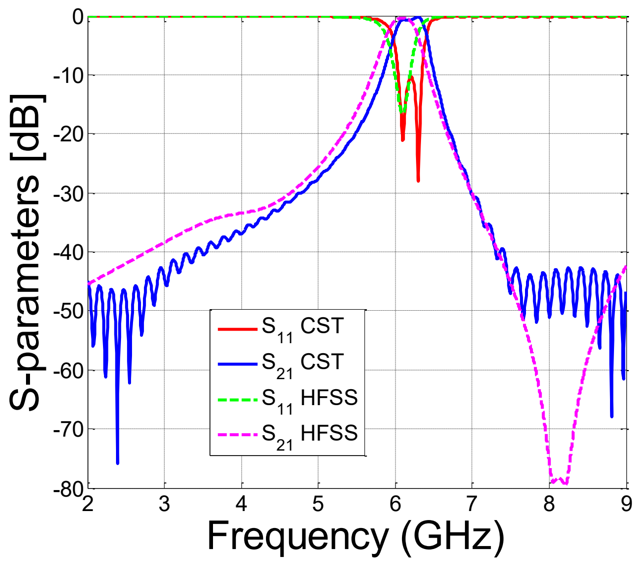

Figure III.6: Simulation results of the reflection and transmission coefficients for SIW BPF loaded with four CHMCs.

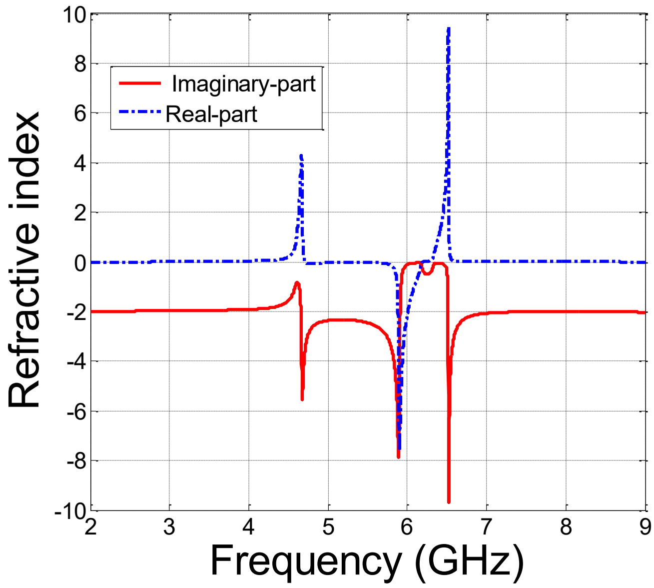

Figure III.7: The real and imaginary parts of the effective refractive index of the SIW BPF loaded with four CHMCs.

Regarding transmission characteristics (Figure III.6), the insertion loss (S21) within the passband, specifically at the 6.2 GHz center frequency, is approximately 1 dB. Outside the passband, the filter demonstrates strong signal rejection capabilities. Maximum attenuation levels reach approximately -75 dB near 2.4 GHz in the lower stopband and -68 dB near 8.8 GHz in the upper stopband.

Complementing the S-parameter analysis, the effective refractive index (n) was again extracted using the NRW method. Figure III.7 shows the resulting real and imaginary parts of ' n ', both displaying negative values across the filter's passband, consistent with the expected metamaterial behavior for this structure as well.

III.4. HMSIW bandpass filters loaded with CHMCs

This section introduces a Bandpass Filter (BPF) design leveraging Half-Mode Substrate Integrated Waveguide (HMSIW) technology as the base structure for loading the proposed Complementary Hexagonal Metamaterial Cells (CHMCs). As detailed earlier in this chapter, HMSIW offers a significant size reduction, achieving approximately 50% of the width of a conventional SIW structure. This is accomplished by replacing one of the lateral via walls with an effective magnetic wall boundary condition, which preserves field properties similar to the full SIW, particularly for the dominant mode whose maximum field intensity is concentrated along the structure's centerline. In this specific design, two identical CHMCs are integrated onto the top conductive layer of the HMSIW. They are separated by a distance X = 5.3 mm, as depicted in Figure III.8. This configuration results in a compact filter footprint of 18.36 mm × 8 mm. Other critical parameters, such as the CHMC geometry and the substrate properties (RT/Duroid 5880, h=0.508 mm), remain consistent with the previously presented designs.

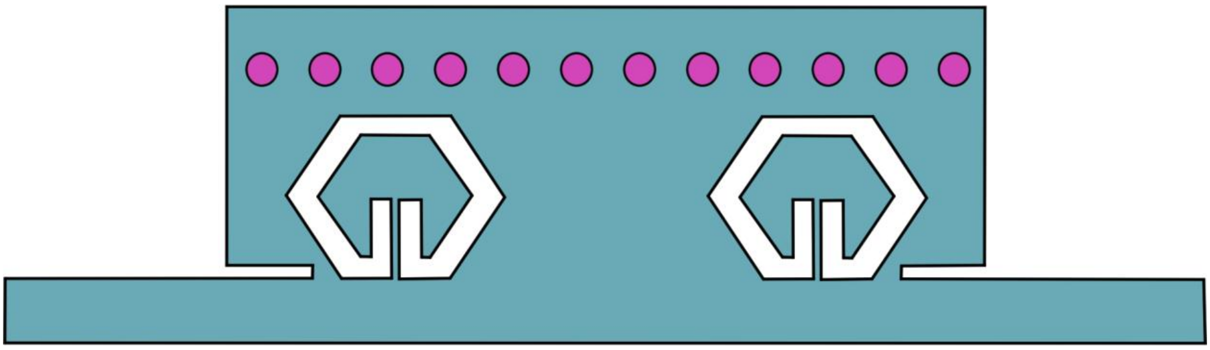

Figure III.8: Upper layer of the HMSIW BPF loaded with two CHMCs.

Figure III.9 presents the simulated S-parameter results (S11 and S21) for the dual-CHMC loaded HMSIW bandpass filter, obtained using [mention simulation tool(s) if consistent, e.g., CST Microwave Studio and validated with HFSS. The simulation indicates well-optimized filter performance. The passband is centered at approximately 6.25 GHz, where the filter exhibits a minimum reflection coefficient (S11) of -35.7 dB and a low insertion loss (S21) below 0.4 dB. The operational bandwidth, defined by S11 < -10 dB, spans from 5.9 GHz to 6.5 GHz. Furthermore, excellent matching (S11 < -20 dB) is achieved within a slightly narrower band from 6.0 GHz to 6.44 GHz. The filter also provides effective out-of-band rejection, with stopbands exhibiting S21 below -10 dB for frequencies below 5.15 GHz and above 6.9 GHz. Notably high rejection levels are observed, reaching approximately -34.5 dB at 2.2 GHz and -69 dB at 7.78 GHz.

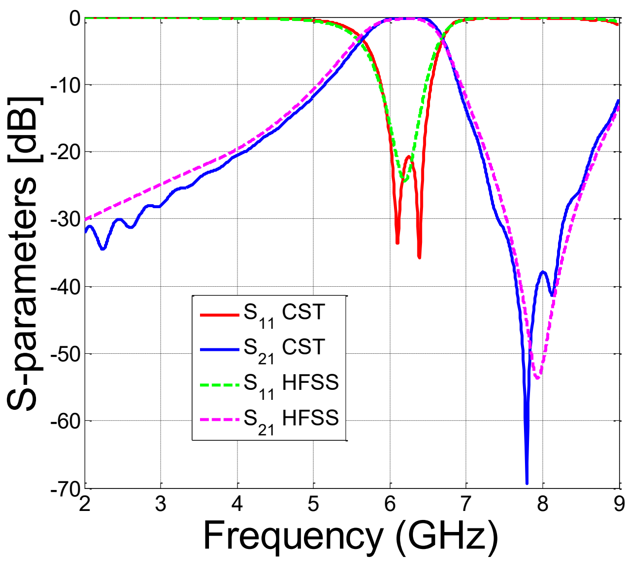

Figure III.9: Simulation results of the S_{11} and S_{21} coefficients for HMSIW bandpass filter loaded with two CHMCs.

To confirm the underlying electromagnetic behavior, the effective refractive index (n) of the HMSIW-based filter was extracted using the NRW retrieval method. Figure III.10 plots the calculated real and imaginary parts of 'n' as a function of frequency. Consistent with the previous designs, both Re (n) and Im (n) exhibit negative values within the filter's operational frequency range (approximately 5.9 GHz to 6.5 GHz). This negative refractive index signature validates the metamaterial nature of the proposed HMSIW filter structure.

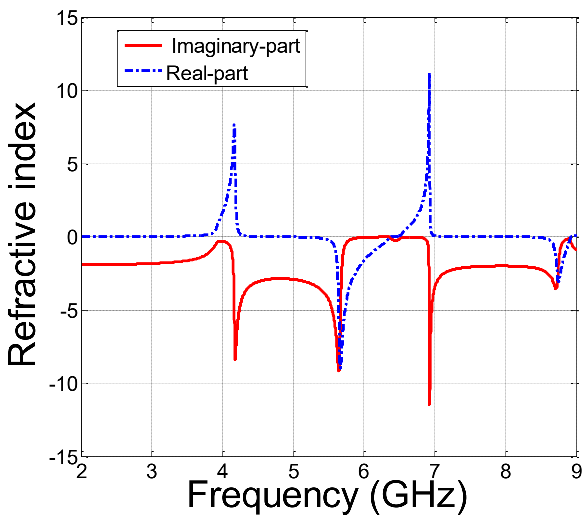

Figure III.10 The real and imaginary parts of the effective refractive index of the HMSIW BPF loaded with two CHMCs.

III.5. Dual-band SIW bandpass filter based on CHMC

A dual-band Bandpass Filter (BPF) is now presented, modifying the initial SIW BPF structure (Figure: III.2). The key difference lies in the two integrated Complementary Hexagonal Metamaterial Cells (CHMCs): instead of being identical, they are designed with distinct sizes (see Figure III-11). This dimensional variation allows each CHMC to target a separate resonant frequency, thereby generating a dual-band response from the overall filter. The specific geometries for the two differing CHMCs are listed in Table III.2. The base SIW structure and substrate remain unchanged from previous examples.

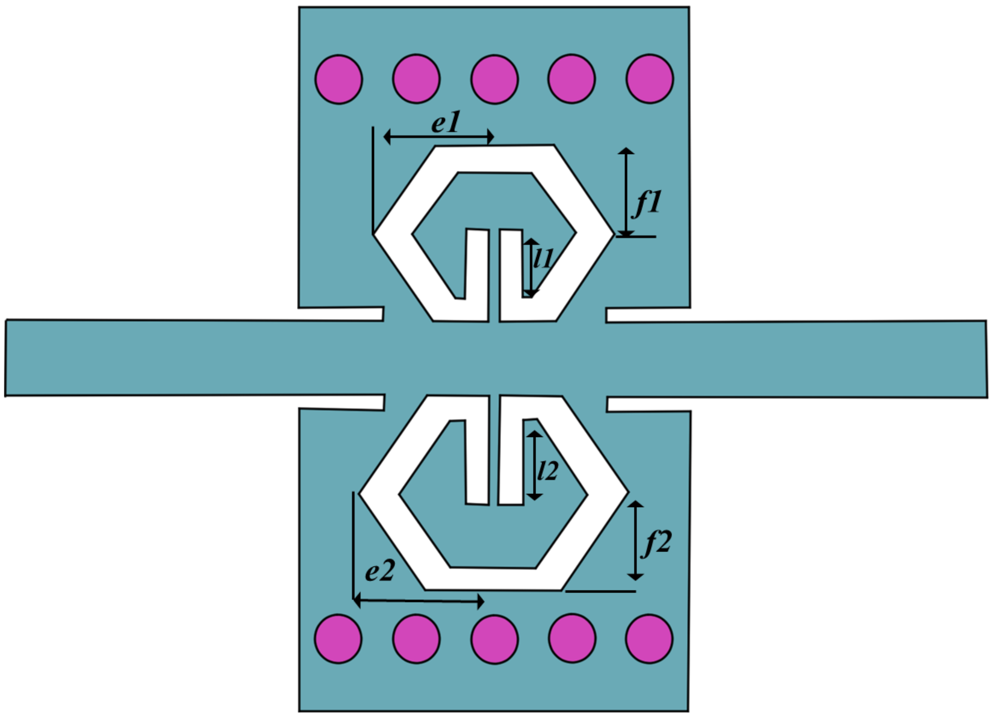

Figure III.11: Top view of the reconfigurable SIW BPF loaded with two different size CHMCs.

Table III.2: The dimensions of each CHMC (unit: mm)

The small CHMC		The big CHMC	
Parameters	**Dimensions**	**Parameters**	**Dimensions**
$e1$	2.5	$e2$	2.8
$f1$	1.8	$f2$	2
$l1$	1.9	$l2$	2.2

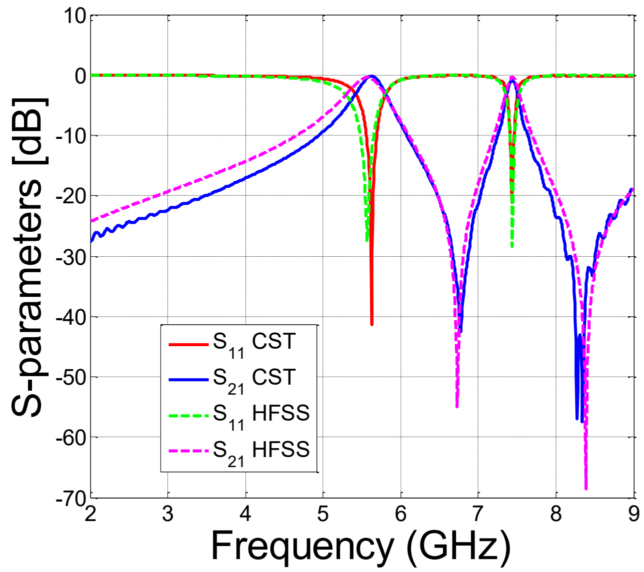

Figure III.12: Simulation results of the S_{11} and S_{21} coefficients of the SIW BPF loaded with two different sizes CHMCs.

Figure III.12 demonstrates the simulated scattering parameters (S11 and S21) for the proposed dual-band Bandpass Filter (BPF) utilizing non-identical CHMCs. The results clearly validate the intended dual-band operation, establishing two distinct passbands centered at approximately 5.6 GHz and 7.4 GHz. Within the first passband (around 5.6 GHz), the filter exhibits excellent performance with a deep reflection coefficient minimum (S11) reaching -40 dB. The second passband (around 7.4 GHz) also shows good matching, with an S11 minimum of -20 dB. Notably, the insertion loss (S21) remains exceptionally low, below 0.1 dB, across both passbands, indicating high transmission efficiency. Furthermore, the filter provides significant signal rejection in the stopbands located below the first passband, between the two passbands, and above the second passband.

The selection of these specific center frequencies, 5.6 GHz and 7.4 GHz, was deliberate, targeting relevant bands within contemporary wireless communication systems. The 5.6 GHz band resides within the widely utilized unlicensed 5 GHz spectrum allocated for Wi-Fi (including IEEE 802.11a/n/ac/ax standards) and is increasingly relevant for unlicensed 5G operations (LTE-U/LAA). Concurrently, the 7.4 GHz frequency aligns with allocations employed for C-band satellite communication uplinks and terrestrial microwave backhaul systems essential for infrastructure connectivity. Therefore, this dual-band BPF design addresses the practical need for compact, integrated microwave components capable of servicing multiple important high-frequency applications within a single device.

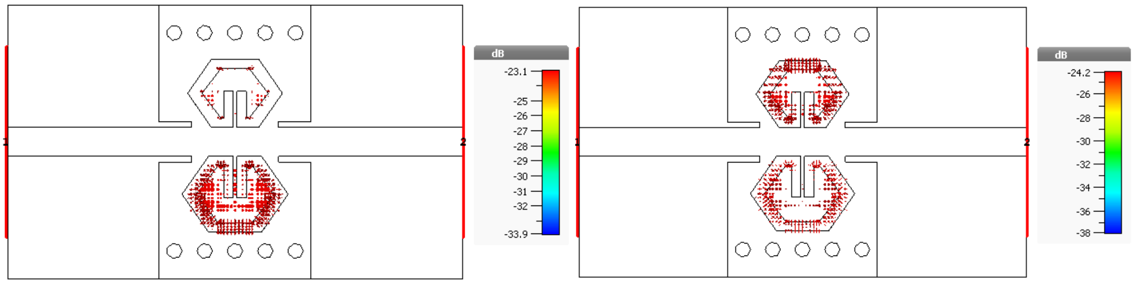

(a) (b)

Figure III.13: E-field distributions: (a) at 5.6 GHz; (b) at 7.4 GHz.

To gain insight into the resonance mechanism of the dual-band filter, the simulated electric field (E-field) distributions at the center frequencies of both passbands are presented in Figure 4.38. At the lower resonance frequency of 5.6 GHz (Figure III.13 (a)), the E-field intensity is observed to be predominantly concentrated within and around the larger of the two Complementary Hexagonal Metamaterial Cells (CHMCs). This localization strongly suggests that the larger CHMC is primarily responsible for establishing the first passband. Conversely, at the higher resonance frequency of 7.4 GHz (Figure III.13 (b)), while the E-field intensity is highest near the smaller CHMC, a noticeable field distribution is also present around the larger CHMC. This indicates that although the smaller CHMC principally governs the second resonance, there is some degree of electromagnetic coupling between the two resonators influencing the characteristics of the second passband.

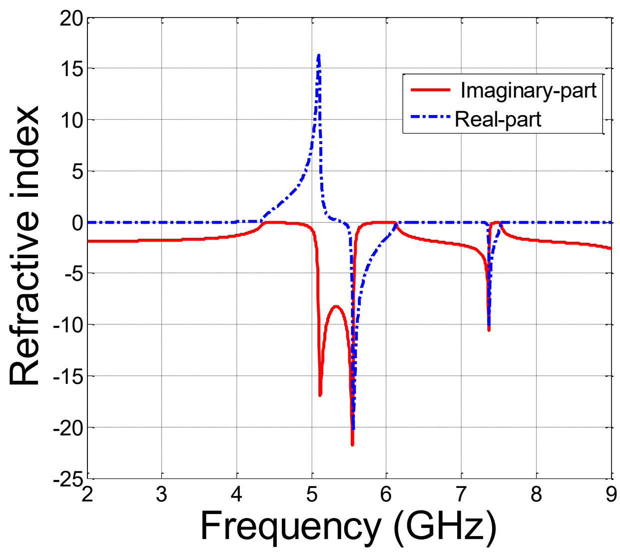

Figure III-14 The real and imaginary parts of the effective refractive index of the dual-mode SIW BPF loaded with two CHMCs.

Further validation of the filter's classification as a metamaterial device is provided by the extracted effective refractive index (n), presented in Figure III.14. Calculated via the NRW technique, both the real and imaginary components of 'n' are found to be concurrently negative in frequency ranges encompassing the two targeted passbands (around 5.6 GHz and 7.4 GHz). This characteristic signature of a negative refractive index across both operational bands confirms the effective metamaterial nature of the dual-band filter.

III.6. General comparison

The preceding sections have detailed the design and performance of four distinct Bandpass Filters (BPFs), all fundamentally based on the integration of the novel Complementary Hexagonal Metamaterial Cell (CHMC) acting as a Defected Ground Structure (DGS) element within either Substrate Integrated Waveguide (SIW) or Half-Mode SIW (HMSIW) platforms. A consistent outcome across all presented designs is the successful realization of effective filtering characteristics, including well-defined passbands with low insertion loss, good return loss, and significant out-of-band rejection. Furthermore, the extraction of effective parameters consistently revealed negative refractive indices within the operational bands, validating the intended metamaterial behavior derived from the CHMC integration.

Despite this common foundation and successful validation, the four filters offer distinct performance profiles tailored for different application requirements. The choice among these configurations' hinges on specific needs regarding operating frequency, required bandwidth, single- versus multi-band operation, and physical size constraints.

- The initial SIW filter with two identical CHMCs serves as a baseline, providing effective narrow-band filtering at a single frequency (5.8 GHz) with moderate miniaturization.
- The SIW filter employing four identical CHMCs demonstrates how increasing resonator count can broaden the passband (around 6.2 GHz) at the expense of increased physical length.
- The HMSIW filter with two identical CHMCs prioritizes miniaturization, achieving a significant reduction in width while offering filtering performance comparable to the SIW versions (around 6.25 GHz), making it suitable for highly space-constrained applications.

- Finally, the SIW filter using two non-identical CHMCs showcases the versatility of the CHMC design by enabling a dual-band response (5.6 GHz and 7.4 GHz), ideal for systems requiring operation across multiple distinct frequency standards within a single component.

III.7. Conclusion

This chapter introduced a novel Complementary Hexagonal Metamaterial Cell (CHMC) and demonstrated its successful application in creating various Bandpass Filters (BPFs) on SIW and HMSIW platforms. Four distinct designs showcased the ability to achieve narrow-band, wider-bandwidth single-band, miniaturized, and dual-band filtering characteristics by manipulating the number, dimensions, and arrangement of the CHMCs. All proposed filters exhibited desirable electromagnetic properties in simulation, including low loss and good rejection. Importantly, their function as effective metamaterials was consistently validated through the extraction of negative refractive indices using the NRW method within their respective operational frequency bands. This work establishes the CHMC as an effective and adaptable element for designing compact microwave filters, offering tailored solutions based on the specific performance trade-offs (size, bandwidth, frequency coverage) required by the target application.

References

[III.1] **T. Saktioto, R. F. Syahputra, S. Punthawanunt, J. Ali, and P. Yupapin,** "GHz frequency filtering source using hexagonal metamaterial splitting ring resonators," Microw. Opt. Technol. Lett., vol. 59, no. 6, pp. 1337–1340, Jun. 2017, doi: 10.1002/MOP.30531.

[III.2] **A. M. Nicolson and G. F. Ross,** "Measurement of the Intrinsic Properties of Materials by Time-Domain Techniques," IEEE Trans. Instrum. Meas., vol. 19, no. 4, pp. 377–382, 1970, doi: 10.1109/TIM.1970.4313932.

[III.3] **W. B. Weir,** "Automatic Measurement of Complex Dielectric Constant and Permeability at Microwave Frequencies," Proc. IEEE, vol. 62, no. 1, pp. 33–36, 1974, doi: 10.1109/PROC.1974.9382.

[III.4] **D. R. Smith, S. Schultz, P. Markoš, and C. M. Soukoulis,** "Determination of effective permittivity and permeability of metamaterials from reflection and transmission coefficients," Phys. Rev. B, vol. 65, no. 19, p. 195104, Apr. 2002, doi: 10.1103/PhysRevB.65.195104.

GENERAL CONCLUSION

General Conclusion

This dissertation successfully addressed the design and analysis of advanced bandpass filters, leveraging the advantageous properties of Substrate Integrated Waveguide (SIW) and Half-Mode SIW (HMSIW) technologies. A central contribution of this work was the introduction, characterization, and application of a novel Complementary Hexagonal Metamaterial Cell (CHMC). Through the strategic integration of these CHMC elements into SIW and HMSIW platforms, a series of bandpass filters were designed and analyzed. The results consistently demonstrated the efficacy of the CHMC in achieving significant filter miniaturization while maintaining desirable electromagnetic characteristics, including low insertion loss and good out-of-band rejection.

The versatility of the proposed CHMC was showcased through the development of various filter configurations, achieving narrow-band, wider-bandwidth single-band, and dual-band responses. This was accomplished by systematically varying the number, dimensions, and arrangement of the CHMC units. Furthermore, the metamaterial behavior of the CHMC-loaded structures was consistently validated through the extraction of negative refractive indices within their respective operational frequency bands. The findings of this study establish the CHMC as an effective and adaptable building block for creating compact, high-performance microwave filters, offering tailored solutions to meet the diverse demands of modern communication systems.

Scope of Future Developments

Building upon the promising results obtained in this study, several avenues for future research and development can be identified:

- **Targeting Different Frequency Bands:** The scalability of the CHMC design could be investigated for operation in other microwave frequency ranges. A particularly interesting direction would be to explore its application towards millimeter-wave (mm-wave) frequencies, where the demand for miniaturization and high performance is even more pronounced and the inherent advantages of SIW/HMSIW become increasingly critical.
- **Designing Multi-Band Filters:** While dual-band filters were presented, future work could focus on designing filters with more complex passband requirements, such as

triple-bandpass filters, by employing multiple CHMC cells with carefully engineered geometries and arrangements to control distinct frequency responses.

- **Application to Other Microwave Components:** The novel CHMC and the design techniques developed in this work could be extended to propose other passive microwave components. A particularly promising area is the design of compact and efficient antennas, where metamaterial-inspired structures have shown considerable potential for enhancing performance parameters such as gain, bandwidth, and radiation pattern control.